Report 48: The value of vaccine booster doses to mitigate the global impact of the Omicron SARS-CoV-2 variant

Alexandra B Hogan[1], Sean L Wu[2], Patrick Doohan[1], Oliver J Watson[1,3], Peter Winskill[1], Giovanni Charles[1], Gregory Barnsley[1], Eleanor M Riley[4], David S Khoury[5], Neil M Ferguson[1], Azra C Ghani[1]

1. MRC Centre for Global Infectious Disease Analysis, Jameel Institute, School of Public Health, Imperial College London, London, UK.
2. Institute for Health Metrics and Evaluation, University of Washington, Seattle, USA
3. London School of Hygiene and Tropical Medicine, London, UK
4. Institute of Immunology and Infection Research, School of Biological Sciences, University of Edinburgh, UK
5. Kirby Institute, University of New South Wales, Sydney, Australia

Summary

Vaccines have played a central role in mitigating severe disease and death from COVID-19 in the past 12 months. However, efficacy wanes over time and this loss of protection will be compounded by the emergence of the Omicron variant. By fitting an immunological model to population-level vaccine effectiveness data, we estimate that neutralizing antibody titres for Omicron are reduced by 4.5-fold (95% CrI 3.1–7.1) compared to the Delta variant. This is predicted to result in a drop in vaccine efficacy against severe disease (hospitalisation) from 96.5% (95% CrI 96.1%–96.8%) against Delta to 80.1% (95% CrI 76.3%–83.2%) against Omicron for the Pfizer-BioNTech booster by 60 days post boost if NAT decay at the same rate following boosting as following the primary course, and from 97.6% (95% CrI 97.4%-97.9%) against Delta to 85.9% (95% CrI 83.1%-88.3%) against Omicron if NAT decay at half the rate observed after the primary course. Integrating this immunological model within a model of SARS-CoV-2 transmission, we show that booster doses will be critical to mitigate the impact of future Omicron waves in countries with high levels of circulating virus. They will also be needed in "zero-COVID" countries where there is little prior infection-induced immunity in order to open up safely. Where dose supply is limited, targeting boosters to the highest risk groups to ensure continued high protection in the face of waning immunity is of greater benefit than giving these doses as primary vaccination to younger age-groups. In all scenarios it is likely that health systems will be stretched. It may be essential, therefore, to maintain and/or reintroduce NPIs to mitigate the worst impacts of the Omicron variant as it replaces the Delta variant. Ultimately, Omicron variant-specific vaccines are likely to be required.

1. Introduction

The rapid development and roll-out of vaccines against SARS-CoV-2 has dramatically altered the course of the global pandemic, substantially reducing COVID-19 cases, hospitalisations, and deaths. Despite high initial vaccine efficacy against wild-type infection, the emergence of variants of concern, in particular the globally prevalent Delta variant, has resulted in a loss of efficacy against mild infection and onward transmission (*1–3*). Recent weeks have seen the emergence of the Omicron variant, exhibiting a large number of mutations in the spike protein gene, and raising concerns that this variant may further evade both infection- and vaccine-induced immune responses (*4*). Alongside this, there is now clear evidence that vaccine efficacy against existing variants wanes over time (*5, 6*). Whilst the extent of waning against severe disease (i.e. that requiring hospitalisation) is less than that against mild disease, even small reductions in protection can result in significant rises in hospitalisations and deaths, particularly in high-risk groups. As a result, many countries are now implementing, or considering, booster programmes. Data on the immunogenicity of booster vaccines are encouraging; for third doses administered between 6- and 8-months post dose 2, neutralizing antibody titres (NAT) increased between 4- and 8-fold compared to NATs measured post dose 2 (*7–9*). Recent data from a clinical trial of the Pfizer-BioNTech vaccine demonstrate a restoration in vaccine efficacy against the Delta variant, reported to be 95% against mild infection (*10*). Similar restoration of efficacy is evident in real-world data from Israel and the UK (*11, 12*). However, the benefit of booster doses in any given population will depend on the current stage of their primary vaccine programme including the supply of vaccine doses, as well as the epidemic that has been experienced to date. Furthermore, the benefits of booster vaccination will depend on the extent to which the Omicron variant replaces the Delta variant and the extent to which Omicron further evades existing immunity. We sought to explore these issues by integrating a model of the dynamics of immunity induced by both infection and vaccines within a population-based virus transmission model.

2. Results

To capture the dynamics of vaccine-induced protection, we followed the approach in (*13*) to describe the relationship between NAT, and protection against mild and severe disease, over time. More recent data on decays in NAT over time after a two-dose vaccination regimen suggest an initial rapid decline (up to 90 days (*14*), in line with the 108-day estimate in (*13*)) with a second slower phase of decay with a half-life of approximately 500 days (*15*). We further re-parameterised the model to incorporate data on NAT and vaccine efficacy following dose 1 from clinical trials (*16–18*), and on the immunogenicity of booster doses delivered between 6- and 8-months post dose 2 (*19*). To capture reduced efficacy against the Omicron variant, we applied a multiplicative scaling factor to reflect reduced neutralization of this variant for all vaccines modelled. Reductions in NATs for previous variants compared to wild type (WT) have been in the range 1.6–8.8 (*20*) whilst early studies have shown between a 6- to 40-fold reduction in NAT relative to WT for Omicron (*21–23*).

We used these data to generate priors (see Table S1) to fit the model to real-world estimates of vaccine efficacy against mild disease (PCR+ tests which include symptomatic cases and asymptomatic infections detected through screening in schools and workplaces), severe disease (hospitalisations) and death (within 28 days of a positive test) with the Delta and Omicron variants from England (*24, 25*). Data were available for two vaccine regimens: Pfizer-BioNTech primary series with Pfizer-BioNTech booster (PF-PF) and Oxford-AstraZeneca (AZ-PF) primary series with PF booster. As demonstrated in the Phase III trials and subsequent population studies for the Delta variant, both vaccine regimens are estimated to generate initial substantial protection against mild and severe disease (Figure 1). The model also captures the observed slower waning of efficacy against severe

disease compared to the faster waning against mild disease, generated by the different dose-response curves fitted to these two endpoints (Figure 1, Figure S1). For these vaccine regimens, we estimate that the boosting with PF (used in both regimens) increases NATs by 1.6-fold (95% credible interval, CrI 1.4–1.9) compared to NATs following dose 2 of PF and 3.3-fold (95% CrI 2.5–4.7) compared to NATs following dose 2 of AZ, resulting in similar NATs following the boost regardless of the primary course. We estimate a 4.5-fold (95% CrI 3.1–7.1) reduction in NATs against the Omicron variant compared to

the Delta variant (20) which translates to approximately a 12–26-fold drop in NAT compared to the ancestral virus (WT), consistent with a meta-analysis of NAT studies (*26*). This drop in NATs matches the observed drop in vaccine efficacy against mild disease. Under this model, we would expect to see a similar drop in vaccine efficacy against severe disease and death, although broader immunological responses may provide protection above those indicated by NAT levels. Furthermore, we expect to see a tail in this distribution meaning a minority who exhibit a poor response to vaccination could be at particularly high risk of severe outcomes (Figure 1, illustrated as individual trajectories).

Table 1 shows the predicted vaccine efficacy against mild disease, severe disease and death following the primary series and a booster dose for these two regimens. Our results suggest that vaccine efficacy against both mild and severe disease could be substantially impacted by the Omicron variant. Under this model, we predict that 60 days after PF boosting efficacy against severe disease will decline from 96.5% (95% CrI 96.1%–96.8%) against Delta to 80.1% (95% CrI 76.3%–83.2%) against Omicron. In making this projection we assume that NATs decay at the same rate following the booster dose as was observed following the primary series and that there is no change in the relationship between NAT and protection. This is likely to be a worst-case scenario as boosting may generate longer lived antibody-producing cells resulting in continuous antibody production over a longer period of time. Assuming that the decay of NATs following the booster occurs at half the rate as following the primary vaccination course increases our predicted vaccine efficacy 60 days post dose 3 to 85.9% (95% CrI 83.1%–88.3%) (Table S4). A more optimistic scenario is one in which the NAT following boost are 6-fold higher than the NATs at dose 2 (as indicated by immunogenicity data although this results in a poorer fit to the vaccine effectiveness data), which would result in 95.6% (92.6% -97.7%) vaccine efficacy against severe disease 90 days post boost (Table S5). We use this optimistic scenario as a sensitivity analysis in our subsequent results. Whilst there remains considerable uncertainty as to the level of protection and its longevity post-boost, all scenarios suggest that either repeated boosts and/or Omicron-variant specific vaccines are likely to be needed to restore protection to the levels seen in Phase III vaccine trials (25).

We used the same approach to capture infection-induced immunity and hence its interaction with vaccine-induced immunity. Cohort studies in high-risk populations suggest that protection against mild infection is consistently maintained at levels above 90% for the first 8–12 months post infection (*27–31*), likely due to the broader immunological response induced by the whole virus compared to the relatively limited response induced by the vaccine (that contains only the spike protein). We capture this by calculating the increase in NAT for an infection that generates 90% mean protection over 1 year. We assume that NATs decay at the same rate as for those induced through vaccination. However, because a substantially higher increase in NAT compared to that estimated from vaccination is required to match 90% protection from re-infection over 1 year (consistent with a recent modelling study (*32*)), this results in our model in a slower decline in protection in those previously infected compared to the protection afforded through vaccination. We assume that infection-induced immunity in NAT to the Omicron variant is reduced to the same extent as vaccine-induced immunity. For our estimated fold-reduction of vaccine-induced immunity to the Omicron variant compared to Delta, this would imply 60% (95% CrI 49%- 70%) mean protection against re-infection from the Omicron

variant over one year, a 33% reduction in protection compared to Delta, consistent with levels reported from South Africa and the UK (*25*, *33*).

In many countries, vaccination is occurring in populations that have already been exposed to past waves of infection and therefore will have developed a substantial level of infection-induced immunity. Studies of the immunogenicity of the PF vaccine in previously infected individuals suggest that a single vaccine dose generates a response similar to or exceeding two vaccine doses in infection naïve individuals (*34*, *35*). This effect is captured in our model, with the first vaccine dose further increasing existing NAT from prior infection.

For both infection- and vaccine-induced immunity, longer-term waning of NAT depends on the rate of loss of long-lived antibody secreting cells. This is captured in our model by the second slower decline, although this rate of decline is uncertain and may be slower after boosting. It is plausible that the degree of waning after infection is slower than that after vaccination, and therefore that high prior levels of infection-induced immunity could provide a higher degree of protection than captured here. It is also likely that aspects of the overall immune response will vary by age; however, there are currently insufficient data to explore the impact of age on waning vaccine efficacy or immune escape from booster doses due to the shorter follow-up in younger populations.

We next considered how booster doses should best be deployed given the current state of the global pandemic. To do so, we developed an individual-based model of SARS-CoV-2 transmission within which we embedded the immunological model (Figure S2, Figure S3). The model is parameterised to capture differences between countries in demography, age-mixing patterns, and health system impacts on access to hospital facilities (*36*, *37*). To capture the different epidemic trajectories that have occurred alongside access to vaccines, we stratify the current epidemiological state of countries into three broad categories.

The first captures countries that have experienced substantial past transmission (and hence have a substantial level of infection-induced immunity) and that also have a high level of access to vaccines. Many high- and upper-middle-income countries fall into this category – including North America, countries in Central/South America, the Middle East and much of Europe. We created a representative epidemic profile for such countries, with a first wave occurring between March and May 2020, a second wave occurring during the northern hemisphere winter of 2020/21, and transmission gradually increasing (i.e. interventions being relaxed) from mid-2021 (Figure S4). We assumed that the primary courses of vaccines (using PF-PF vaccine schedule properties) were administered from January 2021 onwards at a constant rate of 5% of the population dosed per week, a pace that would result in approximately 80% of the population being vaccinated by the end of August 2021 (Figure 2A). Whilst patterns of roll-out have varied between countries, most prioritised the elderly and high-risk individuals initially. We therefore mimicked this prioritisation approach, with the oldest individuals vaccinated first and vaccines delivered sequentially until everyone aged 10 years or above is vaccinated. Throughout we assumed 90% uptake within each age-group.

In countries in which the adult population has already received their primary (2 dose) immunisation, we find that administration of a booster dose (6 months post dose 2) to those aged 60+ years has a substantial impact, reducing deaths by approximately 25% from January 2021 to end-2022 compared to not boosting and assuming no other non-pharmaceutical interventions (NPIs) are in place (Figure 2B–C). This reduction in deaths due to the booster dose is concentrated in the highest risk age-groups (Figure 2D). Due to the timing of the predicted Omicron wave relative to vaccination (Figure 2A), the impact of progressively continuing the booster programme into younger age groups will likely depend on how transmission evolves in 2022, although infections would likely be reduced (Figure S5).

Under our central estimate for the impact of the emergence of the Omicron variant and assuming no change in severity (a plausible worst-case scenario), in the absence of a booster programme we predict a significant winter wave at levels comparable to or exceeding previous waves (Figure 2C) with deaths peaking at approximately 95 per million per day. To mitigate this, high coverage of booster doses is required, particularly in the highest-risk age-groups, but even this is likely to result in a severe strain on health systems (with peak deaths reaching 70 per million per day with high booster coverage in the 60+ age-group). Under a scenario with R_t reaching 5 rather than 7.5 (implying a smaller increase in transmissibility than under our default scenario), the magnitude of this peak would be reduced, reaching 45 per million per day with the 60+ age-groups boosted (Figure 2E). Under our roll-out assumptions, administering boosters at 3 months post dose 2 would bring forward doses in younger groups only (Figure 2A) and would therefore have a moderate impact on reducing infections but less impact on deaths, due to the largest mortality risk being in older age-groups who have already received their booster dose (Figure 2D). In sensitivity analyses, if the vaccine efficacy following boost remains substantially higher than in our central scenario (as would be predicted by a 6-fold increase in NAT compared to dose 2), then we expect to see a peak at similar levels to previous waves (Figure S7). It may be essential, therefore, to maintain and/or reintroduce NPIs to mitigate the worst impacts of the Omicron variant as it replaces the Delta variant.

The second set of countries are those that have experienced substantial prior transmission (and hence have a substantial level of infection-induced immunity) but that to date have had limited access to vaccines. Many low- and lower-middle-income countries fall into this category. In these settings, decisions on future vaccine roll-out are likely to be constrained by limited vaccine supply and/or uptake. To assess the value of boosters we therefore compared two roll-out scenarios. In the first, the primary immunisation (assuming two AZ doses) is delivered to all individuals in the highest risk groups (60+ years) and is then paused before delivering AZ boosters to these same groups at 6 months following dose 2 (for which we assume the same scaling for a booster dose relative to dose 2 as estimated for PF). In the second scenario, we assume that the same number of vaccine doses is instead used to continue primary vaccination into younger age-groups (Figure 3A). The latter results in those aged 40+ years being targeted for two vaccine doses. These vaccine roll-out scenarios were evaluated against the same background epidemic explored in high-income settings (Figure S4), but with a slower pace of vaccine roll-out and lower coverage targets. We find that prioritising limited vaccine supply for boosters in the elderly higher-risk population has a greater public health impact, reducing deaths by an additional 5% compared to using these same doses to immunise younger age-groups in an effort to reduce transmission (Figure 3B-C). Total infections were similar between the two targeting approaches (Figure S8). If vaccine efficacy post-boost remains higher than assumed in our central scenario, prioritising boosters becomes increasingly beneficial (Figure S9). Similar results are obtained if the booster cut-off was chosen as 40+ years rather than 60+ years, with greater overall impact due to the larger number of doses delivered under this scenario (reducing deaths by an additional 15%, Figure S10). The exception is where a slower rollout resulted in vaccination occurring later than the lifting of NPIs, "missing" the epidemic wave (Figure 3D, Figure S8C). Regardless, given the slower pace of vaccine roll-out that has occurred to date in these countries, it is likely that the Omicron variant could result in a large epidemic, likely matching or exceeding previous waves, that could put a significant strain on health systems (Figure 3C). Notably however, this is mitigated in part by the partial immunity afforded by the recent Delta waves and is therefore not predicted to be as large as an epidemic generated in the absence of infection-induced immunity.

The final set of countries are those that successfully interrupted transmission (the so-called "zero-COVID" countries, mostly in east Asia and the Pacific) and therefore have limited infection-induced immunity. These countries face a different challenge, aiming to gradually reopen their borders and

their economies once vaccine coverage is high enough to limit the health impact of increased transmission. In these countries, if NPIs had been relaxed completely once 80% of the adult population had received their primary immunisation (assuming two PF doses, in these simulations representing September 2021), it is likely that they would have experienced a significant Delta wave despite high vaccine coverage (Figure 4, Figure S11). Relaxing interventions following delivery of booster doses to the highest risk 60+ age-group is still likely to generate a large epidemic (comparable to the waves experienced in other countries) due to the reduced vaccine efficacy against Omicron combined with its high transmissibility (Figure 4). Delaying NPI relaxation until the population is fully boosted (here illustrated with an April 2022 relaxation) is however predicted to result in a worse outcome because by this time vaccine efficacy following the booster dose will have waned in the highest-risk groups (Figure 4). This result will be sensitive to the booster vaccine efficacy (Figure S12) and decay following the booster dose. Similarly, if NPIs are relaxed more gradually alongside the scale-up of booster doses across the population, it is possible that significant peaks could still be generated because of waning of vaccine efficacy against Omicron in the highest-risk groups. Countries will therefore need to carefully consider how well protected their vaccinated at-risk populations are when opening up given the lack of infection-induced immunity across the population.

3. Conclusions

Given the rapid spread of the Omicron variant to date, it is now highly likely that this will replace the circulating Delta variant in many countries in the coming weeks. Emerging immunogenicity data clearly point to substantial reductions in NAT whilst preliminary vaccine efficacy estimates demonstrate a substantial reduction in protection from mild disease. Our estimates suggest that this is likely to translate into small but important reductions in efficacy against severe disease and death, although this could be moderated by lower VFR and increased longevity of T cell-mediated immunity compared to NAT in a naïve unvaccinated population. A further remaining uncertainty is how severe the disease caused by the Omicron variant is compared to disease caused by previous variants. However, even if severity is one third of the severity of the Delta variant, we could plausibly expect the peak in hospitalisations and deaths to be similar to the levels encountered in previous waves. Whilst it may take several weeks to fully understand severity, governments need to consider putting mitigations in place now to alleviate any potential impact. Our analyses demonstrate the importance of delivering booster doses as part of the wider public health response to restore vaccine efficacy against the Omicron variant. Prioritising these boosters to high-risk and older populations over primary vaccination in younger age-groups should be part of this response if vaccine dose supply is limited or vaccine roll out delayed.

4. Acknowledgements

5. References

1. J. Lopez Bernal, N. Andrews, C. Gower, E. Gallagher, R. Simmons, S. Thelwall, J. Stowe, E. Tessier, N. Groves, G. Dabrera, R. Myers, C. N. J. Campbell, G. Amirthalingam, M. Edmunds, M. Zambon, K. E. Brown, S. Hopkins, M. Chand, M. Ramsay, Effectiveness of Covid-19 Vaccines against the B.1.617.2 (Delta) Variant. *New England Journal of Medicine*. **385**, 585–594 (2021).

2. O. Tek Ng, V. Koh, C. J. Chiew, K. Marimuthu, N. May Thevasagayam, T. Minn Mak, J. Kiat Chua, S. Si Hui Ong, Y. Kai Lim, Z. Ferdous, A. Khairunnisa bte Johari, M. I-Cheng Chen, S. Maurer-Stroh, L. Cui, R. Tzer Pin Lin, K. Bryan Tan, A. R. Cook, Y.-S. Leo, V. J. Lee, O. Ng, V. Koh, C. Chiew, The Lancet Regional Health-Western Pacific 17 (2021) 100299 The Lancet Regional Health-Western Pacific. **17**, 100299 (2021).

3. A. Singanayagam, S. Hakki, J. Dunning, K. J. Madon, M. A. Crone, A. Koycheva, N. Derqui-Fernandez, J. L. Barnett, M. G. Whitfield, R. Varro, A. Charlett, R. Kundu, J. Fenn, J. Cutajar, V. Quinn, E. Conibear, W. Barclay, P. S. Freemont, G. P. Taylor, S. Ahmad, M. Zambon, N. M. Ferguson, A. Lalvani, Articles Community transmission and viral load kinetics of the SARS-CoV-2 delta (B.1.617.2) variant in vaccinated and unvaccinated individuals in the UK: a prospective, longitudinal, cohort study (2021), doi:10.1016/S1473-3099(21)00648-4.

4. UK Health Security Agency, "SARS-CoV-2 variants of concern and variants under investigation in England" (2021).

5. Y. Goldberg, M. Mandel, Y. M. Bar-On, O. Bodenheimer, L. Freedman, E. J. Haas, R. Milo, S. Alroy-Preis, N. Ash, A. Huppert, Waning Immunity after the BNT162b2 Vaccine in Israel. *New England Journal of Medicine* (2021), doi:10.1056/NEJMoa2114228.

6. H. Chemaitelly, P. Tang, M. R. Hasan, S. AlMukdad, H. M. Yassine, F. M. Benslimane, H. A. al Khatib, P. Coyle, H. H. Ayoub, Z. al Kanaani, E. al Kuwari, A. Jeremijenko, A. H. Kaleeckal, A. N. Latif, R. M. Shaik, H. F. Abdul Rahim, G. K. Nasrallah, M. G. al Kuwari, H. E. al Romaihi, A. A. Butt, M. H. Al-Thani, A. al Khal, R. Bertollini, L. J. Abu-Raddad, Waning of BNT162b2 Vaccine Protection against SARS-CoV-2 Infection in Qatar. *New England Journal of Medicine* (2021), doi:10.1056/nejmoa2114114.

7. R. Yorsaeng, N. Suntronwong, H. Phowatthanasathian, S. Assawakosri, S. Kanokudom, T. Thongmee, P. Vichaiwattana, C. Auphimai, L. Wongsrisang, D. Srimuan, T. Thatsanatorn, S. Klinfueng, N. Sudhinaraset, N. Wanlapakorn, Y. Poovorawan, Immunogenicity of a third dose viral-vectored COVID-19 vaccine after receiving two-dose inactivated vaccines in healthy adults, doi:10.1101/2021.09.16.21263692.

8. R. Sablerolles, W. Rietdijk, A. Goorhuis, D. Postma, L. Visser, D. Geers, K. Schmitz, H. Garcia Garrido, M. Koopmans, V. Dalm, N. Kootstra, A. Huckriede, M. Lafeber, D. van Baarle, C. GeurtsvanKessel, R. de Vries, P. van der Kuy, SWITCH research group, Immunogenicity and reactogenicity of booster vaccinations after Ad26.COV.S priming, doi:10.1101/2021.10.18.21264979doi: medRxiv preprint.

9. B. M. Schultz, F. Melo-González, L. F. Duarte, N. Ms Gálvez, G. A. Pacheco, J. A. Soto, R. v Berríos-Rojas, L. A. González, D. Moreno-Tapia, D. Rivera-Pérez, G. Hoppe-Elsholz, C. Iturriaga, M. Ríos, O. P. Vallejos, M. Urzua, Y. Vázquez, M. S. Navarrete, Á. Rojas, D. Weiskopf, A. Sette, G. Zeng, W. Meng, S. Group, J. v González-Aramundiz, P. A. González, K. Abarca, A. M. Kalergis, S. M. Bueno, A booster dose of an inactivated vaccine increases neutralizing antibodies and T cell responses against SARS-CoV-2, doi:10.1101/2021.11.16.21266350.

10.   Pfizer, Follow-Up Data From Phase 3 Trial of Pfizer-BioNTech COVID-19 Vaccine Support Safety and High Efficacy in Adolescents 12 Through 15 Years of Age | Pfizer, (available at https://www.pfizer.com/news/press-release/press-release-detail/follow-data-phase-3-trial-pfizer-biontech-covid-19-vaccine).

11.   Y. M. Bar-On, Y. Goldberg, M. Mandel, O. Bodenheimer, L. Freedman, N. Kalkstein, B. Mizrahi, S. Alroy-Preis, N. Ash, R. Milo, A. Huppert, Protection of BNT162b2 Vaccine Booster against Covid-19 in Israel. *New England Journal of Medicine*. **385**, 1393–1400 (2021).

12.   N. Andrews, J. Stowe, F. Kirsebom, C. Gower, M. Ramsay, J. Lopez Bernal, Effectiveness of BNT162b2 (Comirnaty, Pfizer-BioNTech) COVID-19 booster vaccine against covid-19 related symptoms in England: test negative case-control study, doi:10.1101/2021.11.15.21266341.

13.   D. S. Khoury, D. Cromer, A. Reynaldi, T. E. Schlub, A. K. Wheatley, J. A. Juno, K. Subbarao, S. J. Kent, J. A. Triccas, M. P. Davenport, Neutralizing antibody levels are highly predictive of immune protection from symptomatic SARS-CoV-2 infection. *Nature Medicine*. **27**, 1205–1211 (2021).

14.   E. H. Y. Lau, O. T. Y. Tsang, D. S. C. Hui, M. Y. W. Kwan, W. hung Chan, S. S. Chiu, R. L. W. Ko, K. H. Chan, S. M. S. Cheng, R. A. P. M. Perera, B. J. Cowling, L. L. M. Poon, M. Peiris, Neutralizing antibody titres in SARS-CoV-2 infections. *Nature Communications*. **12** (2021), doi:10.1038/s41467-020-20247-4.

15.   E. H. Lau, D. S. Hui, O. T. Tsang, W.-H. Chan, M. Y. Kwan, S. S. Chiu, S. M. Cheng, R. L. Ko, J. K. Li, S. Chaothai, C. H. Tsang, L. L. Poon, M. Peiris, Long-term persistence of SARS-CoV-2 neutralizing antibody responses after infection and estimates of the duration of protection. *EClinicalMedicine*. **41**, 101174 (2021).

16.   P. M. Folegatti, K. J. Ewer, P. K. Aley, B. Angus, S. Becker, S. Belij-Rammerstorfer, D. Bellamy, S. Bibi, M. Bittaye, E. A. Clutterbuck, C. Dold, S. N. Faust, A. Finn, A. L. Flaxman, B. Hallis, P. Heath, D. Jenkin, R. Lazarus, R. Makinson, A. M. Minassian, K. M. Pollock, M. Ramasamy, H. Robinson, M. Snape, R. Tarrant, M. Voysey, C. Green, A. D. Douglas, A. V. S. Hill, T. Lambe, S. C. Gilbert, A. J. Pollard, J. Aboagye, K. Adams, A. Ali, E. Allen, J. L. Allison, R. Anslow, E. H. Arbe-Barnes, G. Babbage, K. Baillie, M. Baker, N. Baker, P. Baker, I. Baleanu, J. Ballaminut, E. Barnes, J. Barrett, L. Bates, A. Batten, K. Beadon, R. Beckley, E. Berrie, L. Berry, A. Beveridge, K. R. Bewley, E. M. Bijker, T. Bingham, L. Blackwell, C. L. Blundell, E. Bolam, E. Boland, N. Borthwick, T. Bower, A. Boyd, T. Brenner, P. D. Bright, C. Brown-O'Sullivan, E. Brunt, J. Burbage, S. Burge, K. R. Buttigieg, N. Byard, I. Cabera Puig, A. Calvert, S. Camara, M. Cao, F. Cappuccini, M. Carr, M. W. Carroll, V. Carter, K. Cathie, R. J. Challis, S. Charlton, I. Chelysheva, J. S. Cho, P. Cicconi, L. Cifuentes, H. Clark, E. Clark, T. Cole, R. Colin-Jones, C. P. Conlon, A. Cook, N. S. Coombes, R. Cooper, C. A. Cosgrove, K. Coy, W. E. M. Crocker, C. J. Cunningham, B. E. Damratoski, L. Dando, M. S. Datoo, H. Davies, H. de Graaf, T. Demissie, C. di Maso, I. Dietrich, T. Dong, F. R. Donnellan, N. Douglas, C. Downing, J. Drake, R. Drake-Brockman, R. E. Drury, S. J. Dunachie, N. J. Edwards, F. D. L. Edwards, C. J. Edwards, S. C. Elias, M. J. Elmore, K. R. W. Emary, M. R. English, S. Fagerbrink, S. Felle, S. Feng, S. Field, C. Fixmer, C. Fletcher, K. J. Ford, J. Fowler, P. Fox, E. Francis, J. Frater, J. Furze, M. Fuskova, E. Galiza, D. Gbesemete, C. Gilbride, K. Godwin, G. Gorini, L. Goulston, C. Grabau, L. Gracie, Z. Gray, L. B. Guthrie, M. Hackett, S. Halwe, E. Hamilton, J. Hamlyn, B. Hanumunthadu, I. Harding, S. A. Harris, A. Harris, D. Harrison, C. Harrison, T. C. Hart, L. Haskell, S. Hawkins, I. Head, J. A. Henry, J. Hill, S. H. C. Hodgson, M. M. Hou, E. Howe, N. Howell, C. Hutlin, S. Ikram, C. Isitt, P. Iveson, S. Jackson, F. Jackson, S. W. James, M. Jenkins, E. Jones, K. Jones, C. E. Jones, B. Jones, R. Kailath, K. Karampatsas, J. Keen, S. Kelly, D. Kelly, D. Kerr, S. Kerridge, L. Khan, U. Khan, A. Killen, J. Kinch, T. B. King, L. King, J. King, L. Kingham-Page, P.

Klenerman, F. Knapper, J. C. Knight, D. Knott, S. Koleva, A. Kupke, C. W. Larkworthy, J. P. J. Larwood, A. Laskey, A. M. Lawrie, A. Lee, K. Y. Ngan Lee, E. A. Lees, H. Legge, A. Lelliott, N. M. Lemm, A. M. Lias, A. Linder, S. Lipworth, X. Liu, S. Liu, R. Lopez Ramon, M. Lwin, F. Mabesa, M. Madhavan, G. Mallett, K. Mansatta, I. Marcal, S. Marinou, E. Marlow, J. L. Marshall, J. Martin, J. McEwan, L. McInroy, G. Meddaugh, A. J. Mentzer, N. Mirtorabi, M. Moore, E. Moran, E. Morey, V. Morgan, S. J. Morris, H. Morrison, G. Morshead, R. Morter, Y. F. Mujadidi, J. Muller, T. Munera-Huertas, C. Munro, A. Munro, S. Murphy, V. J. Munster, P. Mweu, A. Noé, F. L. Nugent, E. Nuthall, K. O'Brien, D. O'Connor, B. Oguti, J. L. Oliver, C. Oliveira, P. J. O'Reilly, M. Osborn, P. Osborne, C. Owen, D. Owens, N. Owino, M. Pacurar, K. Parker, H. Parracho, M. Patrick-Smith, V. Payne, J. Pearce, Y. Peng, M. P. Peralta Alvarez, J. Perring, K. Pfafferott, D. Pipini, E. Plested, H. Pluess-Hall, K. Pollock, I. Poulton, L. Presland, S. Provstgaard-Morys, D. Pulido, K. Radia, F. Ramos Lopez, J. Rand, H. Ratcliffe, T. Rawlinson, S. Rhead, A. Riddell, A. J. Ritchie, H. Roberts, J. Robson, S. Roche, C. Rohde, C. S. Rollier, R. Romani, I. Rudiansyah, S. Saich, S. Sajjad, S. Salvador, L. Sanchez Riera, H. Sanders, K. Sanders, S. Sapaun, C. Sayce, E. Schofield, G. Screaton, B. Selby, C. Semple, H. R. Sharpe, I. Shaik, A. Shea, H. Shelton, S. Silk, L. Silva-Reyes, D. T. Skelly, H. Smee, C. C. Smith, D. J. Smith, R. Song, A. J. Spencer, E. Stafford, A. Steele, E. Stefanova, L. Stockdale, A. Szigeti, A. Tahiri-Alaoui, M. Tait, H. Talbot, R. Tanner, I. J. Taylor, V. Taylor, R. te Water Naude, N. Thakur, Y. Themistocleous, A. Themistocleous, M. Thomas, T. M. Thomas, A. Thompson, S. Thomson-Hill, J. Tomlins, S. Tonks, J. Towner, N. Tran, J. A. Tree, A. Truby, K. Turkentine, C. Turner, N. Turner, S. Turner, T. Tuthill, M. Ulaszewska, R. Varughese, N. van Doremalen, K. Veighey, M. K. Verheul, I. Vichos, E. Vitale, L. Walker, M. E. E. Watson, B. Welham, J. Wheat, C. White, R. White, A. T. Worth, D. Wright, S. Wright, X. L. Yao, Y. Yau, Safety and immunogenicity of the ChAdOx1 nCoV-19 vaccine against SARS-CoV-2: a preliminary report of a phase 1/2, single-blind, randomised controlled trial. *The Lancet*. **396**, 467–478 (2020).

17.   E. E. Walsh, R. W. Frenck, A. R. Falsey, N. Kitchin, J. Absalon, A. Gurtman, S. Lockhart, K. Neuzil, M. J. Mulligan, R. Bailey, K. A. Swanson, P. Li, K. Koury, W. Kalina, D. Cooper, C. Fontes-Garfias, P.-Y. Shi, Ö. Türeci, K. R. Tompkins, K. E. Lyke, V. Raabe, P. R. Dormitzer, K. U. Jansen, U. Şahin, W. C. Gruber, Safety and Immunogenicity of Two RNA-Based Covid-19 Vaccine Candidates. *New England Journal of Medicine*. **383**, 2439–2450 (2020).

18.   N. Imai, A. B. Hogan, L. Williams, A. Cori, T. D. Mangal, P. Winskill, L. K. Whittles, O. J. Watson, E. S. Knock, M. Baguelin, P. N. Perez-Guzman, K. A. M. Gaythorpe, R. Sonabend, A. C. Ghani, N. M. Ferguson, Interpreting estimates of coronavirus disease 2019 (COVID-19) vaccine efficacy and effectiveness to inform simulation studies of vaccine impact: a systematic review. *Wellcome Open Research*. **6**, 185 (2021).

19.   World Health Organisation, Considerations in boosting COVID vaccine immune responses., (available at https://www.who.int/news-room/events/detail/2021/08/13/default-calendar/who-consultation-on-covid-19-vaccines-research-13-august-2021).

20.   D. Cromer, M. Steain, A. Reynaldi, T. E. Schlub, A. K. Wheatley, J. A. Juno, S. J. Kent, J. A. Triccas, D. S. Khoury, M. P. Davenport, Neutralising antibody titres as predictors of protection against SARS-CoV-2 variants and the impact of boosting: a meta-analysis. *The Lancet Microbe* (2021), doi:10.1016/S2666-5247(21)00267-6.

21.   D. J. Sheward, C. Kim, A. Pankow, X. Castro Dopico, D. Martin, J. Dillner, G. B. Karlsson Hedestam, J. Albert, B. Murrell, "Preliminary Report-Early release, subject to modification Quantification of the neutralization resistance of the Omicron Variant of Concern," (available at https://www.who.int/news/item/26-11-2021-classification-of-omicron-).

22.   S. Cele, L. Jackson, K. Khan, D. Khoury, T. Moyo-Gwete, H. Tegally, C. Scheepers, D. Amoako, F. Karim, M. Bernstein, G. Lustig, D. Archary, M. Smith, Y. Ganga, Z. Jule, K. Reedoy, J. Emmanuel San, S.-H. Hwa, J. Giandhari, J. M. Blackburn, A. Sigal, "SARS-CoV-2 Omicron has extensive but incomplete escape of Pfizer BNT162b2 elicited neutralization and requires ACE2 for infection," (available at https://covdb.stanford.edu/page/mutation-viewer/#sec_b-1-351).

23.   Pfizer and BioNTech Provide Update on Omicron Variant | Pfizer, (available at https://www.pfizer.com/news/press-release/press-release-detail/pfizer-and-biontech-provide-update-omicron-variant).

24.   N. Ferguson, A. Cori, D. Laydon, K. Gaythorpe, A. Hogan, N. Imai, W. Hinsley, M. Baguelin, N. Andrews, R. Fitzjohn, G. Nedjati-Gilani, S. Edward, L. Whittles, P. Perez-Guzman, R. Sonabend, A. Ghani, J. Lopez Bernal, Effectiveness of SARS-CoV-2 vaccines in England in 2021: a whole population survival analysis. *Preprint* (2021), doi:https://doi.org/10.25561/93035.

25.   N. Ferguson, A. Ghani, A. Cori, A. Hogan, W. Hinsley, E. Volz, Growth and immune escape of the Omicron SARS-CoV-2 Variant of Concern in England. *Preprint* (2021), doi:https://doi.org/10.25561/93038.

26.   D. S. Khoury, M. Steain, J. A. Triccas, A. Sigal, M. P. Davenport, D. Cromer, Analysis: A meta-analysis of Early Results to predict Vaccine efficacy against Omicron, doi:10.1101/2021.12.13.21267748.

27.   A. Leidi, F. Koegler, R. Dumont, R. Dubos, M. E. Zaballa, G. Piumatti, M. Coen, A. Berner, P. D. Farhoumand, P. Vetter, P. N. Vuilleumier, L. Kaiser, D. Courvoisier, A. S. Azman, I. Guessous, S. Stringhini, H. Baysson, P. Collombet, D. de Ridder, P. d'Ippolito, M. D. asaro A. Rinella, Y. Dibner, N. el Merjani, N. Francioli, M. Frangville, K. Marcus, C. Martinez, N. Noel, F. Pennacchio, J. Perez-Saez, D. Petrovic, A. Picazio, A. Pishkenari, J. Portier, C. Pugin, B. Rakotomiaramanana, A. Richard, L. Salzmann-Bellard, S. Schrempft, Z. Waldmann, A. Wisniak, A. Davidovic, J. Duc, J. Guérin, F. Lombard, M. Will, A. Flahault, I. A. Vernez, O. Keiser, L. Mattera, M. Schellongova, I. Eckerle, P. Lescuyer, B. Meyer, G. Poulain, N. Vuilleumier, S. Yerly, F. Chappuis, S. Welker, L. Gétaz, M. Nehme, F. Pardo, G. Violot, S. Hurst, P. Matute, J. M. Maugey, D. Pittet, A. G. L'Huillier, K. M. Posfay-Barbe, J. F. Pradeau, M. Tacchino, D. Trono, Risk of reinfection after seroconversion to SARS-CoV-2: A population-based propensity-score matched cohort study. *Clinical Infectious Diseases* (2021), doi:10.1101/2021.03.19.21253889.

28.   L. J. Abu-Raddad, H. Chemaitelly, P. Coyle, J. A. Malek, A. A. Ahmed, Y. A. Mohamoud, S. Younuskunju, H. H. Ayoub, Z. al Kanaani, E. al Kuwari, A. A. Butt, A. Jeremijenko, A. H. Kaleeckal, A. N. Latif, R. M. Shaik, H. F. Abdul Rahim, G. K. Nasrallah, H. M. Yassine, M. G. al Kuwari, H. E. al Romaihi, M. H. Al-Thani, A. al Khal, R. Bertollini, SARS-CoV-2 antibody-positivity protects against reinfection for at least seven months with 95% efficacy. *EClinicalMedicine*. **35**, 100861 (2021).

29.   F. Gallais, P. Gantner, T. Bruel, A. Velay, D. Planas, M. J. Wendling, S. Bayer, M. Solis, E. Laugel, N. Reix, A. Schneider, L. Glady, B. Panaget, N. Collongues, M. Partisani, J. M. Lessinger, A. Fontanet, D. Rey, Y. Hansmann, L. Kling-Pillitteri, O. Schwartz, J. de Sèze, N. Meyer, M. Gonzalez, C. Schmidt-Mutter, S. Fafi-Kremer, Evolution of antibody responses up to 13 months after SARS-CoV-2 infection and risk of reinfection. *EBioMedicine*. **71** (2021), doi:10.1016/j.ebiom.2021.103561.

30.   J. Wei, P. C. Matthews, N. Stoesser, T. Maddox, L. Lorenzi, R. Studley, J. I. Bell, J. N. Newton, J. Farrar, I. Diamond, E. Rourke, A. Howarth, B. D. Marsden, S. Hoosdally, E. Y. Jones, D. I. Stuart,

D. W. Crook, T. E. A. Peto, K. B. Pouwels, A. S. Walker, D. W. Eyre, T. Thomas, D. Cook, D. Ayoubkhani, R. Black, A. Felton, M. Crees, J. Jones, L. Lloyd, E. Sutherland, E. Pritchard, K.-D. Vihta, G. Doherty, J. Kavanagh, K. K. Chau, S. B. Hatch, D. Ebner, L. M. Ferreira, T. Christott, W. Dejnirattisai, J. Mongkolsapaya, S. Cameron, P. Tamblin-Hopper, M. Wolna, R. Brown, R. Cornall, G. Screaton, K. Lythgoe, D. Bonsall, T. Golubchik, H. Fryer, S. Cox, K. Paddon, T. James, T. House, J. Robotham, P. Birrell, H. Jordan, T. Sheppard, G. Athey, D. Moody, L. Curry, P. Brereton, I. Jarvis, A. Godsmark, G. Morris, B. Mallick, P. Eeles, J. Hay, H. VanSteenhouse, J. Lee, S. White, T. Evans, L. Bloemberg, K. Allison, A. Pandya, S. Davis, D. I. Conway, M. MacLeod, C. Cunningham, Anti-spike antibody response to natural SARS-CoV-2 infection in the general population. *Nature Communications*. **12**, 6250 (2021).

31. S. Lumley, D. O'Donnell, N. Stoesser, P. Matthews, A. Howarth, S. Hatch, B. Marsden, S. Cox, T. James, F. Warren, L. Peck, T. Ritter, Z. de Toledo, L. Warren, D. Axten, R. Cornall, E. Jones, D. Stuart, G. Screaton, D. Ebner, S. Hoosdally, M. Chand, Oxford University Hospitals Staff Testing Group, D. Crook, A. O'Donnell, C. Conlon, K. Pouwels, A. Walker, T. Peto, S. Hopkins, T. Walker, Jeffery K, D. Eyre, Antibodies to SARS-CoV-2 are associated with protection against reinfection.

32. J. A. Cohen, R. M. Stuart, K. Rosenfeld, H. Lyons, M. White, C. C. Kerr, D. J. Klein, M. Famulare, Quantifying the role of naturally- and vaccine-derived neutralizing antibodies as a correlate of protection against COVID-19 variants, doi:10.1101/2021.05.31.21258018.

33. J. R. C. Pulliam, C. van Schalkwyk, N. Govender, A. von Gottberg, C. Cohen, M. J. Groome, J. Dushoff, K. Mlisana, H. Moultrie, Increased risk of SARS-CoV-2 reinfection associated with emergence of the Omicron variant in South Africa, doi:10.1101/2021.11.11.21266068.

34. C. Manisty, A. D. Otter, T. A. Treibel, Á. McKnight, D. M. Altmann, T. Brooks, M. Noursadeghi, R. J. Boyton, A. Semper, J. C. Moon, Antibody response to first BNT162b2 dose in previously SARS-CoV-2-infected individuals. *The Lancet*. **397** (2021), pp. 1057–1058.

35. R. A. Urbanowicz, T. Tsoleridis, H. J. Jackson, L. Cusin, J. D. Duncan, J. G. Chappell, A. W. Tarr, J. Nightingale, A. R. Norrish, A. Ikram, B. Marson, S. J. Craxford, A. Kelly, G. P. Aithal, A. Vijay, P. J. Tighe, J. K. Ball, A. M. Valdes, B. J. Ollivere, "Two doses of the SARS-CoV-2 BNT162b2 vaccine enhance antibody responses to variants in individuals with prior SARS-CoV-2 infection" (2021), (available at https://www.science.org).

36. P. G. T. Walker, C. Whittaker, O. J. Watson, M. Baguelin, P. Winskill, A. Hamlet, B. A. Djafaara, Z. Cucunubá, D. O. Mesa, W. Green, H. Thompson, S. Nayagam, K. E. C. Ainslie, S. Bhatia, S. Bhatt, A. Boonyasiri, O. Boyd, N. F. Brazeau, L. Cattarino, G. Cuomo-Dannenburg, A. Dighe, C. A. Donnelly, I. Dorigatti, S. L. van Elsland, R. Fitzjohn, H. Fu, K. A. M. Gaythorpe, L. Geidelberg, N. Grassly, D. Haw, S. Hayes, W. Hinsley, N. Imai, D. Jorgensen, E. Knock, D. Laydon, S. Mishra, G. Nedjati-Gilani, L. C. Okell, H. J. Unwin, R. Verity, M. Vollmer, C. E. Walters, H. Wang, Y. Wang, X. Xi, D. G. Lalloo, N. M. Ferguson, A. C. Ghani, "The impact of COVID-19 and strategies for mitigation and suppression in low-and middle-income countries," (available at https://www.science.org).

37. A. B. Hogan, P. Winskill, O. J. Watson, P. G. T. Walker, C. Whittaker, M. Baguelin, N. F. Brazeau, G. D. Charles, K. A. M. Gaythorpe, A. Hamlet, E. Knock, D. J. Laydon, J. A. Lees, A. Løchen, R. Verity, L. K. Whittles, F. Muhib, K. Hauck, N. M. Ferguson, A. C. Ghani, Within-country age-based prioritisation, global allocation, and public health impact of a vaccine against SARS-CoV-2: A mathematical modelling analysis. *Vaccine*. **39**, 2995–3006 (2021).

38.   A. P. S. Munro, L. Janani, V. Cornelius, P. K. Aley, G. Babbage, D. Baxter, M. Bula, K. Cathie, K. Chatterjee, K. Dodd, Y. Enever, K. Gokani, A. L. Goodman, C. A. Green, L. Harndahl, J. Haughney, A. Hicks, A. A. van der Klaauw, J. Kwok, V. Libri, M. J. Llewelyn, A. C. McGregor, A. M. Minassian, P. Moore, M. Mughal, Y. F. Mujadidi, J. Murira, O. Osanlou, R. Osanlou, D. R. Owens, M. Pacurar, A. Palfreeman, D. Pan, T. Rampling, K. Regan, S. Saich, J. Salkeld, D. Saralaya, S. Sharma, R. Sheridan, A. Sturdy, E. C. Thomson, S. Todd, C. Twelves, R. C. Read, S. Charlton, B. Hallis, M. Ramsay, N. Andrews, J. S. Nguyen-Van-Tam, M. D. Snape, X. Liu, S. N. Faust, COV-BOOST study group, Safety and immunogenicity of seven COVID-19 vaccines as a third dose (booster) following two doses of ChAdOx1 nCov-19 or BNT162b2 in the UK (COV-BOOST): a blinded, multicentre, randomised, controlled, phase 2 trial. *Lancet (London, England)* (2021), doi:10.1016/S0140-6736(21)02717-3.

39.   N. Andrews, J. Stowe, F. Kirsebo, S. Toffa, T. Rickeard, E. Gallagher, C. Gower, M. Kall, N. Groves, A. O'Connell, D. Simons, P. Blomquist, G. Dabrera, R. Myers, S. Ladhani, G. Amirthalingam, S. Gharbia, J. Barrett, R. Elson, N. Ferguson, M. Zambon, C. Campbell, K. Brown, S. Hopkins, M. Chand, M. Ramsay, J. Lopez Bernal, Effectiveness of COVID-19 vaccines against the Omicron (B.1.1.529) variant of concern, doi:10.1101/2021.11.15.21266341.

40.   G. Charles, S. Wu, individual: An R package for individual-based epidemiological models. *Journal of Open Source Software*. **6**, 3539 (2021).

41.   A. Karlinsky, D. Kobak, Tracking excess mortality across countries during the covid-19 pandemic with the world mortality dataset. *eLife*. **10** (2021), doi:10.7554/eLife.69336.

6. Tables

Table 1: Estimated vaccine efficacy against mild disease, severe disease and death for the AZ-PF and PF-PF vaccine regimens as a function of time since dose 2 or booster. Estimates are shown for the Delta variant and the Omicron variant. Values shown are the posterior median and 95% credible intervals. pd2 = post dose 2; pb = post booster.

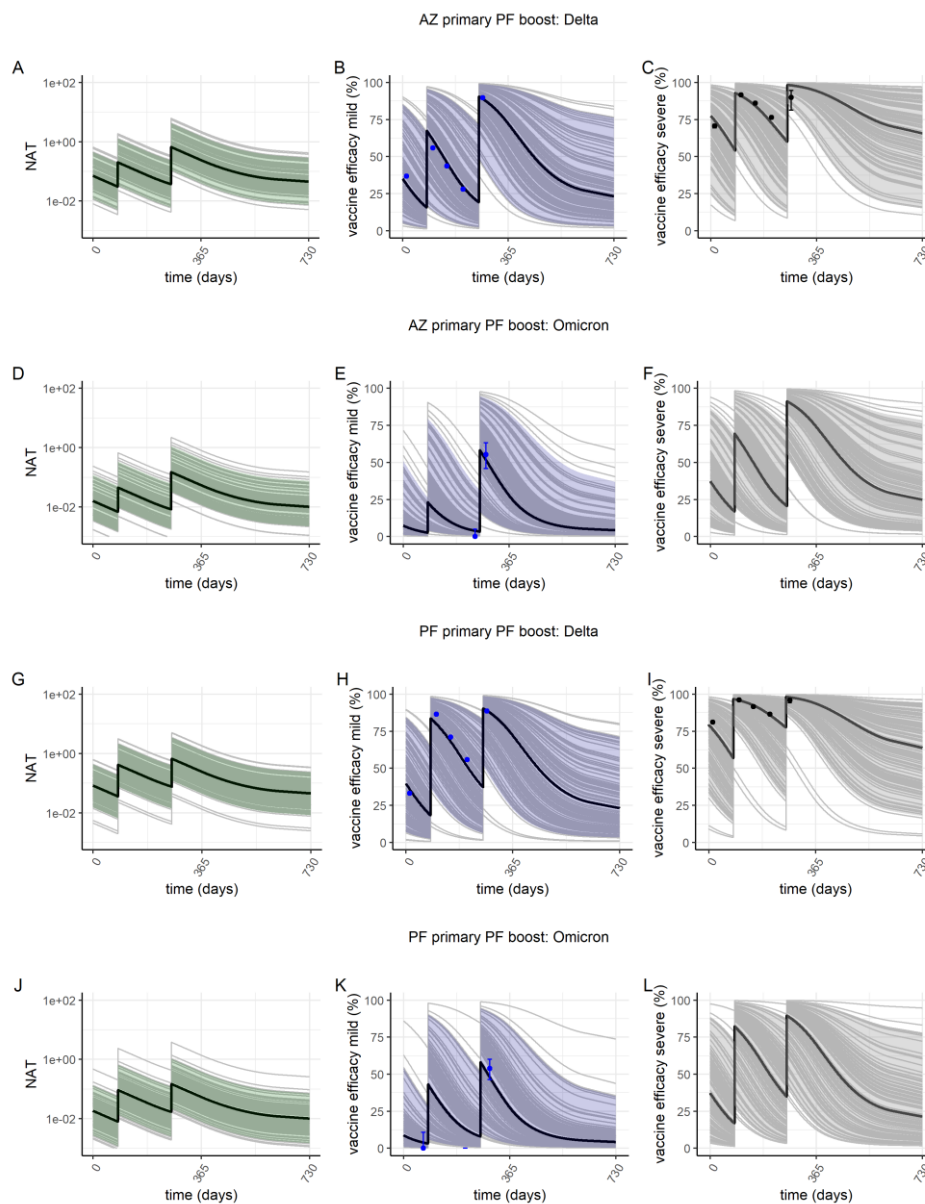| Vaccine	Variant	90d pd2	180d pd2	30d pb	60d pb	90d pb
Efficacy against mild disease						
AZ-PF	Delta	39 (37.9-40.6)	18.9 (17.3-22.2)	86.4 (85.4-87.4)	81.2 (79.7-82.7)	74.7 (72.4-76.8)
AZ-PF	Omicron	8.6 (7.1-10.6)	3.3 (2.7-4.4)	48.4 (43.1-53.5)	38.9 (33.9-44)	30.2 (25.8-35)
PF-PF	Delta	61.6 (60.2-62.9)	36.9 (34.3-41.3)	86.4 (85.4-87.4)	81.2 (79.7-82.7)	74.7 (72.4-76.8)
PF-PF	Omicron	19.1 (15.9-22.7)	7.9 (6.4-10.2)	48.4 (43.1-53.5)	38.9 (33.9-44)	30.2 (25.8-35)
Efficacy against severe disease						
AZ-PF	Delta	80.2 (79.4-81.3)	59.6 (57.1-64.3)	97.6 (97.4-97.8)	96.5 (96.1-96.8)	94.9 (94.3-95.5)
AZ-PF	Omicron	37.3 (32.3-42.9)	17.8 (14.8-22.4)	85.5 (82.6-87.9)	80.1 (76.3-83.2)	73.2 (68.6-77.3)
PF-PF	Delta	91 (90.5-91.5)	78.7 (76.7-81.7)	97.6 (97.4-97.8)	96.5 (96.1-96.8)	94.9 (94.3-95.5)
PF-PF	Omicron	59.8 (54.3-65.1)	35.2 (30-41.7)	85.5 (82.6-87.9)	80.1 (76.3-83.2)	73.2 (68.6-77.3)
Efficacy against death						
AZ-PF	Delta	88.3 (87.7-89.1)	73.4 (71.2-77.1)	98.7 (98.6-98.8)	98.1 (97.9-98.3)	97.2 (96.9-97.5)
AZ-PF	Omicron	52.6 (47.1-58.4)	28.9 (24.5-35.1)	91.7 (89.9-93.2)	88.3 (85.8-90.3)	83.7 (80.4-86.5)
PF-PF	Delta	95 (94.6-95.3)	87.4 (86-89.3)	98.7 (98.6-98.8)	98.1 (97.9-98.3)	97.2 (96.9-97.5)
PF-PF	Omicron	73.6 (68.9-77.7)	50.4 (44.6-57.4)	91.7 (89.9-93.2)	88.3 (85.8-90.3)	83.7 (80.4-86.5)

7. Figures

Figure 1: Predicted vaccine efficacy over time. Plots show neutralizing antibody titre (NAT) (green), vaccine efficacy against mild disease (purple) and severe disease (grey) for the AZ-PF regimen (panels A-F) and PF-PF regimen (panels F–L). The solid black line shows the posterior median estimate, colour bands the 95% range of individual responses and grey lines show 100 individual draws from the variation estimated between individuals in (*13*) illustrating the impact of variability in immune responses across the population. In panels B, E, H and K, the blue points are estimates of vaccine efficacy against mild disease (i.e. PCR+ tested infections which include asymptomatic infections detected through regular screening in schools and some workplaces) with the Delta and Omicron variants in England from (*24, 25*). In panels C and I, the black points represent vaccine efficacy against hospitalisation with the Delta variant from the same source. Panels A–C and G–I show NAT and vaccine efficacy against the Delta variant; panels D–F and J–L show NAT and vaccine efficacy against the Omicron variant.
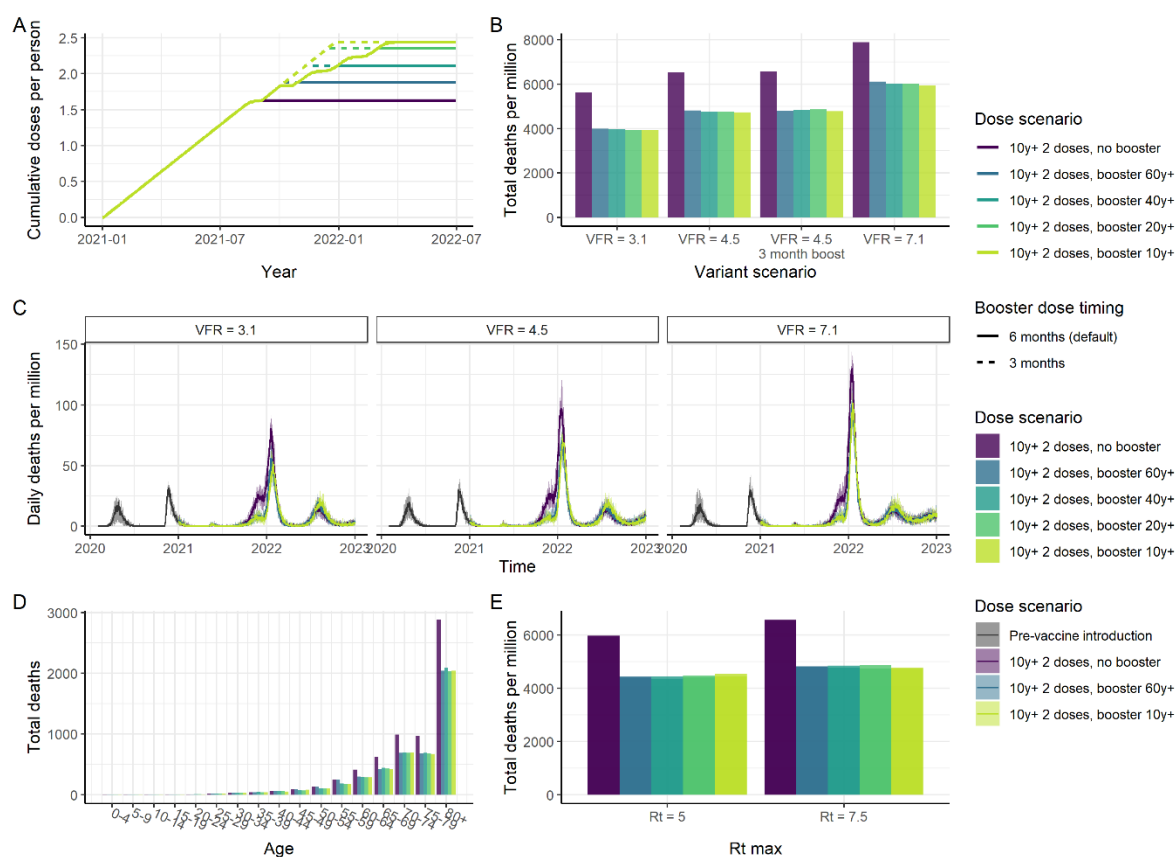
Figure 2: Impact of vaccination in a high-income country setting with substantial prior transmission and high vaccine access. A) Cumulative vaccine doses delivered per person over time, for the category 1 analysis (high-income countries with substantial prior transmission and high vaccine access). Solid lines represent a 6-month period between dose 2 and the booster dose; dashed lines represent a 3-month period. Vaccine impact is shown for five scenarios: no booster doses, booster doses to those aged 60+, booster doses to those aged 40+, booster doses to those aged 20+ and booster doses to those aged 10+. All scenarios assume 90% vaccine uptake in each group. B) Total deaths per million post vaccine introduction at the beginning of 2021 through to end-2022, for the central, upper, and lower VFR estimates, and assuming a 6-month period between dose 2 and the booster, except where specified. C) Daily deaths per million for the lower, central, and upper VFR estimate and assuming R_t reaches 7.5. D) Total deaths per million stratified by 5-year age-group, for the central VFR scenario and assuming R_t reaches 7.5. E) Total deaths per million over the same time period, for two scenarios for the increased transmissibility of the Omicron variant (expressed as the maximum Rt) for our central estimate of immune escape of the Omicron variant.
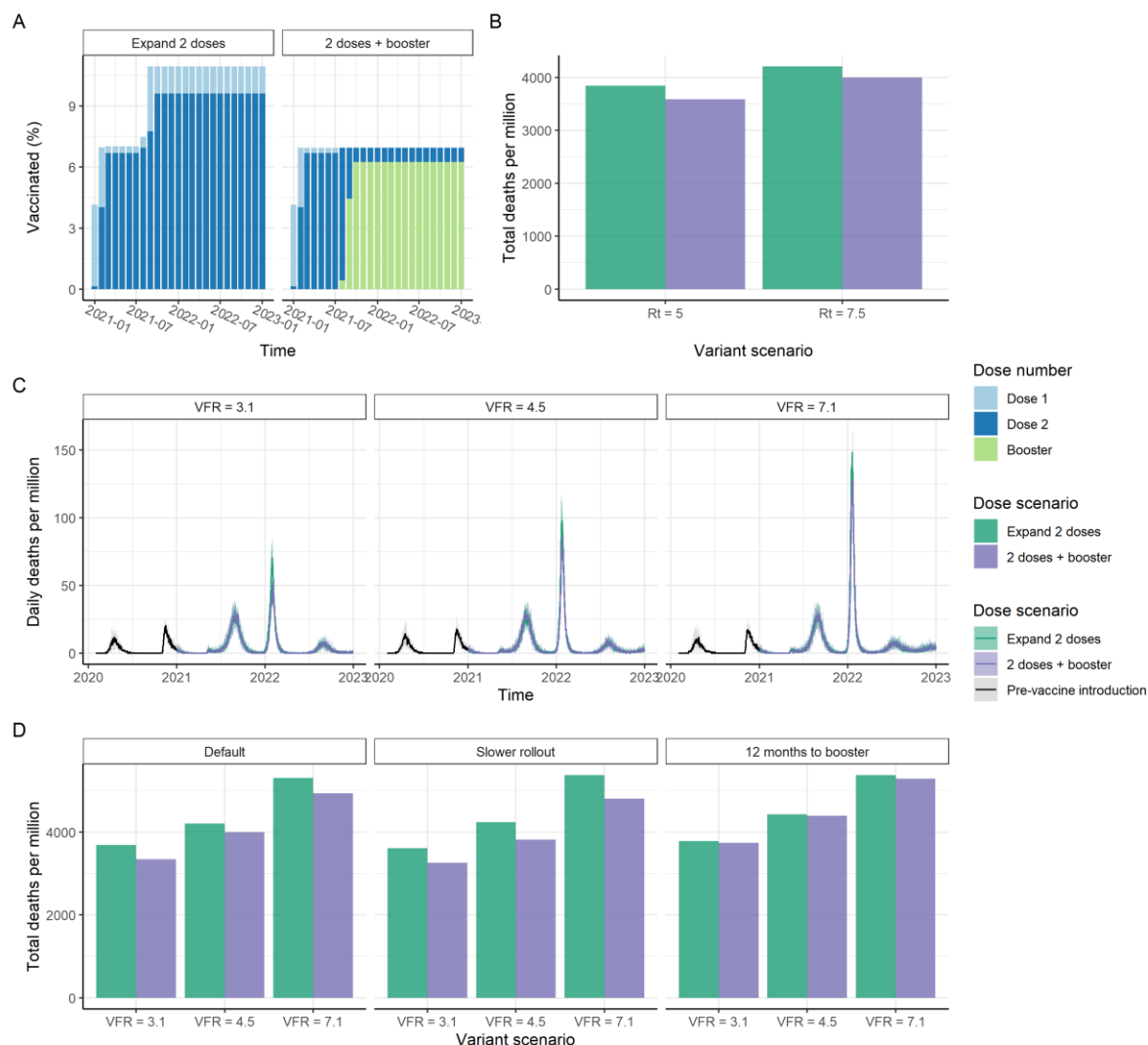
Figure 3: Impact of vaccination in a low-middle-income country setting with substantial prior transmission and low vaccine access, where individuals 60+ years are targeted. Two strategies for distributing a limited vaccine supply are shown (assuming AZ is used for both the primary and booster doses). In the first ("Expand 2 doses"), no booster doses are administered, and the supply is therefore delivered to a wider proportion of the population. In the second ("2 doses + booster") the same supply is delivered to the 60+ age-group (2 dose primary immunisation and booster dose 6 months post dose 2) and no younger groups receive the primary series. A) Cumulative proportion of the population having dose 1 (light blue), dose 2 (dark blue) and the booster (green) each month. B) Total deaths per million post vaccine introduction at the beginning of 2021 through to end-2022, for two scenarios for the increased transmissibility of the Omicron variant (expressed as the maximum R_t) for our central estimate of immune escape of the Omicron variant. C) Daily deaths per million population assuming R_t increases to 7.5. for the central, upper, and lower VFR estimates. D) Total deaths per million population from the start of vaccination in 2021 to end-2022 for the three VFR parameters. Total deaths are shown for the default vaccine rollout (2% of the population per dose per week) and booster dose scenario (180 days post dose 2, "Default"), as well as assuming a slower rollout (1% per week, "Slower rollout") or a one-year gap between dose 2 and the booster ("12 months to booster"). Results for the scenario where the 40+ years population is initially targeted are shown in Figure S10.
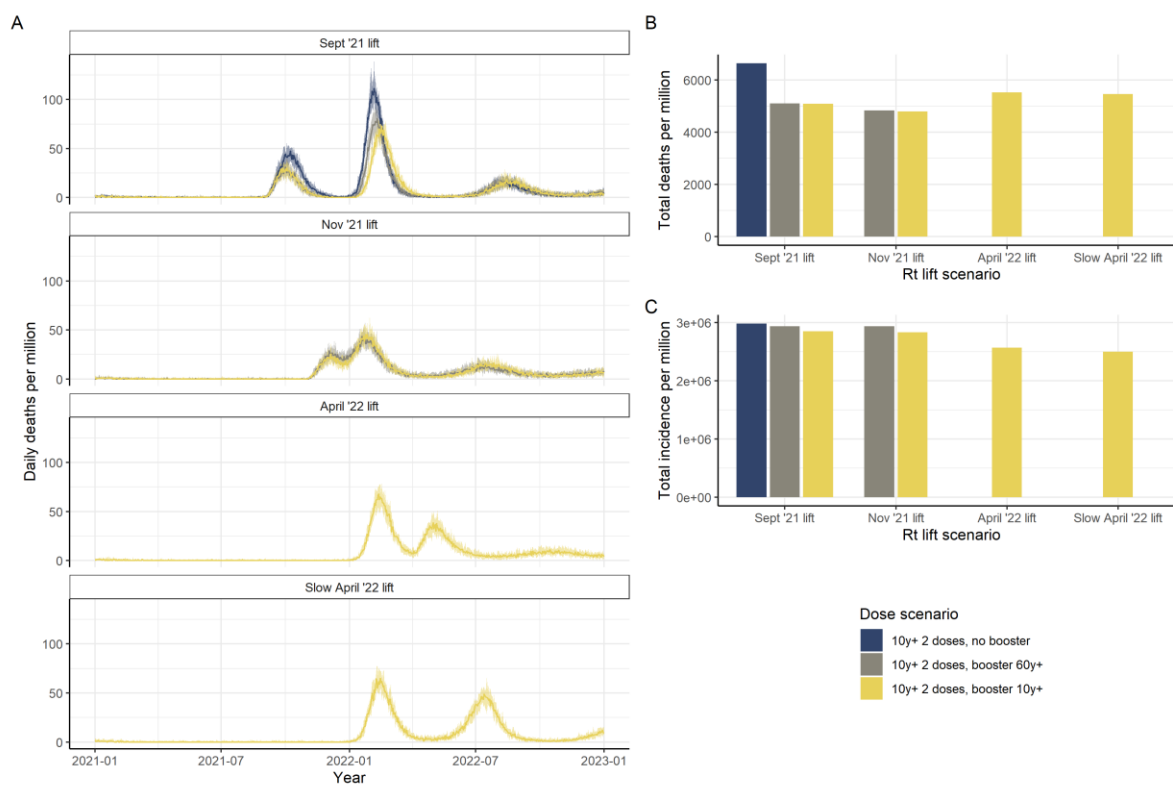
Figure 4: Impact of vaccination in a high-income country setting with minimal prior SARS-CoV-2 transmission and high vaccine access. A) Daily deaths per million population for the scenario where 80% of the population is immunised (2 doses) before NPIs are lifted (i.e. R_t increases). Following Rt increasing ("Sept '21 lift"), vaccination continues at a population dose rate of 5% per week until 90% uptake is achieved in the 10+ years population (brown); boosters are administered to the 60+ years population 6 months post dose 2 (dark blue); or boosters are administered to the 10+ years population (yellow). Additional panels show the impact of lifting NPIs after boosters are given to 60+ years ("Nov '21 lift") or after boosters are given to 10+ years ("April '22 lift" representing a lifting over a one-month period; "Slower April '22 lift" representing lifting over a four-month period). The central VFR estimate and a maximum transmission of $R_t = 7.5$ are applied. Panels B and C show the total deaths and total incidence respectively, per million population from the start of vaccination in 2021 to end-2022, for each scenario.

8. Methods

Immunological Model

To capture the dynamics of vaccine-induced and infection-induced protection, we followed the approach of Khoury et al. (*13*) by considering the relationship between neutralizing antibody titres (NAT) over time, and protection against mild disease (which we assume to be the same as protection against any infection) and against severe disease requiring hospitalisation. We first model each individual's NAT over time, which is based on exponential decay

$$n(t) = n_{ij}e^{-\lambda t},$$

where n_{ij} is the initial NAT of vaccine *i* drawn from a $\log_{10}$-normal distribution at dose *j* and λ is the decay rate. We then assume an initial period of fast antibody decay, representing the combined biochemical decay of antibodies and the ongoing production of antibodies by circulating plasma cells, followed by a second period of linear decrease in decay rate λ and a third period of slow decay, representing the long-lived plasma cells. We assume a logistic relationship between NAT and efficacy to capture time-varying vaccine protection against infection, severe disease and death ($E(t)$), given by the function

$$E(t) = \frac{1}{1 + e^{-k[log_{10}(n(t)) - log_{10}(n_{50})]}},$$

where k is the fitted shape parameter and n_{50} is the NAT relative to convalescent NAT required to provide 50% protection (from infection, severe disease, or death).

Khoury *et al* (*13*) obtained parameters for this model of vaccine-induced protection by fitting to efficacy data from Phase III trials, using NAT data following dose 2 which are based on the mean 28-day values reported in clinical trials relative to the mean titre for a convalescent individual. By definition, on this scale, the NAT induced by infection in convalescent individuals is 1.

However, the parameters from Khoury *et al*. (*13*) are based on trials conducted during the early period of the pandemic and prior to the emergence of variants. To obtain appropriate estimates for the Delta and Omicron variants and to better inform the parameters determining waning, we re-fitted the model to data on vaccine efficacy from a population-wide study in England (*24*, *25*). This study provides estimates of vaccine efficacy for two vaccine regimens over time – Pfizer-BioNTech primary and Pfizer-BioNTech boost, and Oxford-AstraZeneca primary with Pfizer-BioNTech boost – based on data linkage generating a whole population cohort.

We fitted the model to the estimated vaccine efficacies against the two vaccine regimens and for the Delta and Omicron variants using Bayesian methods and assuming a Binomial likelihood for the vaccine efficacy estimates. We used prior estimates from the original model papers to inform our fitting.

To obtain prior estimates for the impact of a booster dose, we collated reported data on immunogenicity from booster trials undertaken between 3- and 8-months following dose 2 (*19*, *38*). Across these studies, the level of the boost relative to dose 2 NAT differed depending on the vaccine and the VOC. For wild-type, the studies reported a 4–5-fold boost after the booster dose compared to dose 2. However, for the Beta variant this appears to be 10–20 fold higher, whilst for Delta the boost

was in the range 5–7 fold compared to dose 2. We thus used a 6-fold boost a prior mean compared to dose 2.

Our priors and their sources are summarised in Table S1. Dose parameters and titre parameters were transformed to the log10 scale, all other parameters were fitted on a linear scale. We used Normal distribution priors on these scales with mean and standard deviations shown in Table S1. Model fitting was undertaken using MCMC methods in the Dr.Jacoby R package (https://mrc-ide.github.io/drjacoby/index.html).

Table S1: Prior and Posterior Parameter Estimates for Immunological Model

Parameter	Symbol	Prior Mean	Prior S.D.	Posterior Estimate – median (95% credible interval)	Reference for Prior Mean
NAT against Delta for dose 1 of the AstraZeneca vaccine relative to convalescent	$n_{AZ,1}$	0.5* $n_{AZ,2}$	0.5	0.07 (0.037, 0.137)	-
NAT against Delta for dose 2 of the AstraZeneca vaccine relative to convalescent	$n_{AZ,2}$	32/59 for WT from data in (*13*) With fold-reduction applied	0.25	0.202 (0.116, 0.361)	(*13, 20*)
Fold-reduction for Delta relative to WT for AstraZeneca vaccine	-	3.9	1.5	2.7 (1.5, 4.7)	(*20*)
NAT for dose 1 of the Pfizer vaccine against Delta	$n_{PF,1}$	0.5* $n_{PF,2}$	0.5	0.081 (0.043, 0.156)	-
NAT for dose 2 of the Pfizer vaccine against Delta	$n_{PF,2}$	223/94 from data in (*13*) With fold-reduction applied	0.25	0.415 (0.235, 0.728)	(*13, 20*)
Fold-increase in NAT for booster dose of Pfizer vaccine against Delta compared to dose 2 of Pfizer	$n_{PF,3}$	6	4	1.6 (1.4, 1.9)	(*19, 38*)
Fold-increase in NAT for booster dose of Pfizer vaccine against Delta compared to dose 2 of AstraZeneca	$n_{AZ,3}$	6	4	3.3 (2.5, 4.7)	(*19, 38*)
Fold-reduction for Delta relative to WT for Pfizer vaccine	-	3.9	1.5	5.7 (3.3, 10.1)	(*20*)
Fold-reduction for Omicron relative to Delta	VFR	10.0	10.0	4.5 (3.1, 7.1)	(*21, 22*)
Titre relative to convalescent required to provide 50% protection from infection	n_{i50}	0.20	0.25	0.113 (0.063, 0.210)	(*13*)
Titre relative to convalescent required to provide 50%	n_{s50}	0.03	0.25	0.027 (0.011, 0.059)	(*13*)

protection from severe disease					
Titre relative to convalescent required to provide 50% protection from death	n_{d50}	0.03	0.25	0.016 (0.006, 0.039)	Assumed the same as hospitalisation
Shape parameter	k	2.94	1	2.9 (2.3, 3.7)	(*13*)
Standard deviation of individual responses		0.44	Not fitted	-	(*13*)
Half-life of antibody decay: short (days)	h_s	90	20	69 (54, 88)	(*13, 14*)
Half-life of antibody decay: long (days)	h_l	500	100	431 (242, 650)	(*15*)
Time period of fast decay (days)	t_s	90	20	95 (66, 119)	(*14*)
Time point relative to dose by which slow decay achieved (days)	t_l	365	80	366 (218, 524)	(*13*)

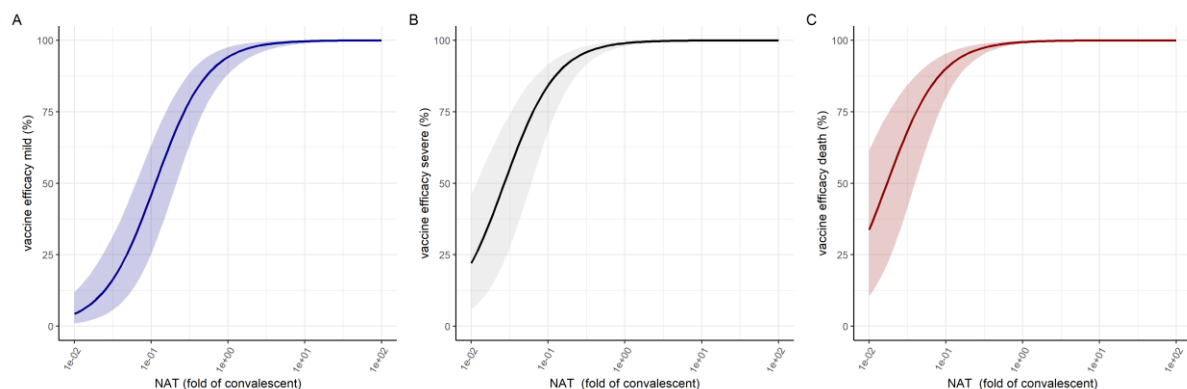The resulting dose-response curves relating NAT to vaccine efficacy are shown in Figure S1.

Figure S1: Dose-response curves estimated from fitting to vaccine efficacy data for the relationship between NAT (fold of convalescent) (x-axis) and vaccine efficacy against mild disease (A), severe disease (B) and death (C). The solid lines are the posterior median estimates and colour bands the 95% credible interval.

The model is fitted to one homologous regimen – PF primary and booster – and one heterologous regimen – AZ primary and PF booster. Data were estimates of vaccine efficacy at time points following either dose 1, dose 2 or the booster dose. We removed observations within the first 21 days post dose 1-, or 14-days post dose 2 or the boost and shifted the time respectively such that day 0 was either 21 or 14 days after the dosing, as our model does not capture the gradual increase in NAT over this short time-period.

As a sensitivity analysis, we re-fit the same model to the vaccine efficacy estimates for England generated using a different design – specifically a test-negative case control (TNCC) study (*12, 39*) . Although derived from the same underlying data, the different control group results in slightly different vaccine efficacy estimates (Figure S6).

We used the same process to capture infection-induced immunity derived from past infections. At each exposure, the NAT are assumed to be boosted by 3.8 with this parameter back calculated from the efficacy curves to give 90% protection against re-infection under our model as indicated from

empirical studies. Each exposure or vaccine dose results in an additive increase in NAT. We imposed an upper limit of exp(5.0) for the total NAT an individual could achieve to represent an arbitrary biological limit.

For the forward simulations we assume that dose 2 is given 28 days following dose 1, whilst the booster dose is given 6 months following dose 2. As we only consider homologous vaccination in the simulations, we assumed that the boost for AZ is the same multiplier of AZ dose 2 as the estimated boost for PF is compared to PF dose 2.

Population Model

To explore the population impact of vaccines, we developed a stochastic, individual-based model (IBM) of SARS-CoV-2 transmission and vaccination ("safir"), including both vaccine-derived and infection-induced immune dynamics. The structure and epidemiology of the model broadly mirrors a previously published compartmental model (*37*) but implements these processes at the individual level to allow more flexible vaccine strategies to be implemented. The simulation updates on a discrete time step, but the specific size of the time step is under user control and can be made arbitrarily small, subject to computational constraints (we use a time-step of 0.2 days here). The model is implemented in R and C++, using the "individual" package to specify and run the simulation (*40*) and is open-source, with full details available at https://mrc-ide.github.io/safir/.

Within the IBM, each individual is assigned a 5-year age bin according to the demographics of the population, and transmission (force of infection) depends on a setting-specific age-structured contact matrix and also the baseline contact rate, which may be time-varying. In addition, infection from external (unmodelled) sources can be included to represent infectious contact with persons outside the modelled population (Figure S2). The states are:

- S = uninfected and therefore susceptible to infection
- E = exposed to infection but not yet infectious
- I_{mild} = infected and infectious with mild symptomatic infection that does not require hospitalisation
- $I_{asymptomatic}$ = infected and infectious with asymptomatic infection that does not require hospitalisation
- I_{case} = infected and infectious with disease that will require hospitalisation
- I_{hosp} = individuals in hospital, which is comprised of:
  - Mechanical ventilation = persons requiring mechanical ventilation
  - Oxygen = persons requiring oxygen
  - Neither = neither
- R = infections and cases that have recovered and are immune to re-infection
- D = cases that have died

Transitions between epidemiological states are summarised in Figure S2, with natural history parameters for SARS-CoV-2 infection, and age-stratified probabilities of requiring hospital care and the infection fatality ratio as reported in Hogan et al. (*37*).
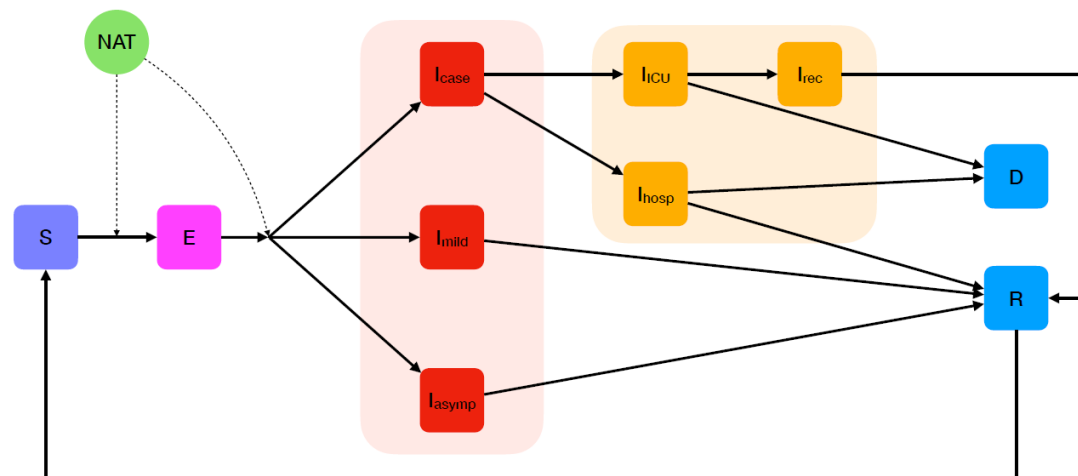
Figure S2: Schematic representation of the compartmental epidemiology of the stochastic IBM. The green circle denotes the neutralising antibody titres (NAT) for each individual which are tracked over time and influence the probability of being infected (from susceptible S to exposed E) and of developing disease requiring hospitalisation (Icase) given a breakthrough infection. Imild denotes mild symptomatic disease, Iasymp asymptomatic infection, Ihosp disease requiring hospitalisation, IICU disease requiring ICU admission, Irec stepdown from ICU, D death, R recovered.

In addition, as described above, each individual stores a real-valued (floating point) log antibody titre value, which is altered by vaccination and infection. Upon receiving a vaccine dose, an individual's NAT is drawn from a vaccine-specific $\log_{10}$-normal distribution and stored for that person. Each person's NAT decays linearly on a natural log scale, as described above.

In addition to vaccination, individuals receive an increase in NAT due to infection (instead of modelling temporary complete immunity as in previous compartmental models, where a person transitions into recovered "R" compartment where they dwell before returning to a susceptible "S" state). In the IBM, upon completion of the disease progression (when a person would have previously transitioned into the "R" compartment), the NAT derived from prior infection is added to that from vaccination (and vice versa) and stored for that individual, thereby capturing the interaction between past infection and vaccination (or vice versa). Because the NAT from infection is added to any existing vaccine-derived NAT, it decays according to the same decay profile.

Subsequent vaccine doses are correlated within individuals, meaning that subsequent antibody boosts from doses are equal to the random initial draw multiplied by the ratio of the previous mean dose-specific NAT to this dose-specific value. This allows us to implicitly capture individual level heterogeneity in immune response to vaccination. This new vaccine dose NAT is added to the current NAT for that individual. We further calculate the residual decayed NAT from the prior vaccine dose (calculated by subtracting the total decay on a natural log scale from the dose-specific logged NAT for the previous dose), and subtract this from the new vaccine dose NAT, so as to accurately implement the NAT profiles in Figure 1 within the IBM.

An individual's antibody titre is used to calculate protection as described above (capturing infection-induced immunity and vaccine-induced immunity in combination). We model protection against infection by reducing the probability that susceptible individuals transition to exposed, and

protection against severe disease by reducing the probability of severe outcomes after being infected.

Vaccine Allocation

Vaccines are allocated according to an algorithm that accounts for available vaccine stock, the age-groups that are prioritised for this dose (and, optionally, future doses), minimum time delays between the receipt of subsequent doses, and coverage targets for each dose and for each age-group. The algorithm is similar to a previously published model (*37*) but generalised for an arbitrary number of doses and booster priority.

For each dose, we specify a matrix of coverage targets by age-group (columns) where rows are ordered prioritisation steps. Elements of the matrix thus identify for each step what target percentage dose coverage of that age-group needs to be fulfilled. We identify what dose is being distributed by distribution "phase" (e.g. on phase 2, the 2nd dose is being distributed). Within that distribution phase, the coverage target matrix specific to that dose/phase is used to distribute doses (subject to availability) according to each row of the matrix. When all coverage targets of a particular prioritisation step (a row) are fulfilled, the distribution algorithm moves to the next step (i.e. the next row). When coverage targets for all steps in a particular dose are achieved, we may move on to the next dose phase (i.e. distribute the next dose).

On each day for which there are at least some available doses, the algorithm checks which priority stage in a phase it is on. If a phase is completed, it advances to the next phase. If not, based on the targets for that step, the set of eligible persons to receive that dose is identified. This considers which age-groups have not yet met coverage targets, and which persons have had an adequate waiting period since their last dose (if phase > 1). Then doses are distributed to those individuals, subject to supply. If there are surplus doses remaining, the algorithm checks whether any age-groups are prioritised for phase + 1 booster doses, and distributes those doses. If any doses remain, they are given out to age-groups in subsequent prioritisation steps. The algorithm stops if all targets for all doses are filled. The flowchart in Figure S3 describes how the algorithm functions on a single day.
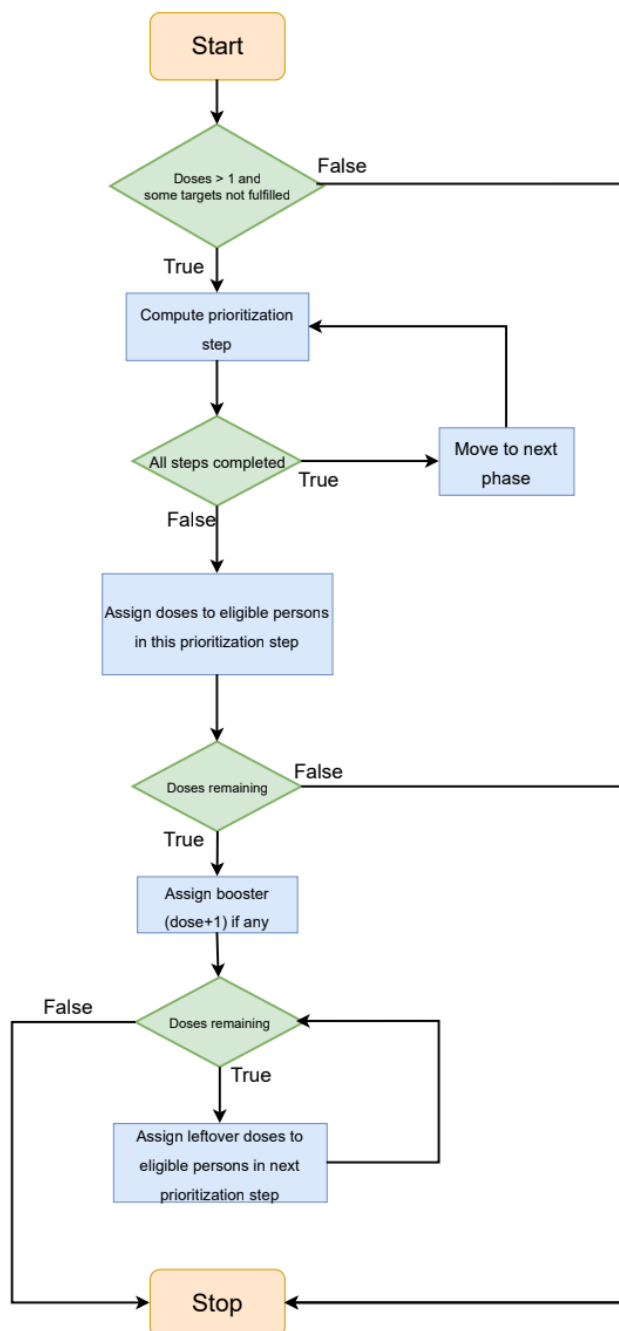
Figure S3: Schematic diagram illustrating the COVID-19 vaccine allocation algorithm.

Forward Simulations

Following the methodology of previous work (*36*, *37*) we consider vaccine impact in four income settings: high-income, upper-middle-income, lower-middle-income, and low-income (HIC, UMIC, LMIC, and LIC, respectively). We characterise each setting by contact pattern, using a typified contact matrix for each income setting (*36*, *37*) and demography, using the age distribution of the country with the median GDP in each income setting (HIC: Malta; UMIC: Grenada; LMIC: Nicaragua; and LIC: Madagascar). We further consider that in LMIC and LIC countries, healthcare system capacity may be limited, and assume that once modelled hospitalised cases exceed a threshold in these settings, infected individuals experience worse outcomes, as in Walker et al (*36*). In HIC and UMIC settings, we assume that healthcare systems are unconstrained.

Modelled transmission is allowed to vary over time by setting a time-varying reproduction number, R_t. Because the types and impacts of NPIs vary depending on setting, rather than modelling any specific NPIs (such as social distancing measures, mask-wearing, or school closures), we assume that the impact of these measures is reflected in the reproduction number. For the country settings in categories 1 and 2 (countries with substantial prior transmission before the rollout of vaccination), we construct a representative trajectory of transmission by varying R_t between 0.8 and 4 (Delta variant), and by increasing R_t up to 7.5 (Omicron variant), such that an initial epidemic wave occurs between March and May 2020, a second wave occurs during December 2020 and January 2021, and transmission gradually increases from mid-2021 (Figure S4). In an HIC setting, this initial trajectory results in approximately 1,700 deaths per million by the end of 2020, which approximately aligns with the excess mortality experienced in high-burden high-income countries(*41*). For the country settings in category 3 (countries with minimal prior transmission before the rollout of vaccination), we construct a representative trajectory such $R_t < 1$ (no sustained transmission) until September 2021, at which point R_t increases gradually to either 4 (Delta variant) or from November 2021 to 7.5 for the Omicron variant (see below). We further explore scenarios in this category where transmission is suppressed until either November 2021, or April 2022, to allow different vaccination strategies to be implemented before NPIs are lifted (Figure 2A).

For the analysis in category 1 (HIC and UMIC countries), we model the rollout of vaccines to individuals starting at 80+ years, down to 10+ years, in consecutive 5-year age-groups, at a constant rate of 5% of the population receiving one dose per week, starting at 1 January 2021, with 90% uptake in each age-group. We then either cease to administer any additional doses ("10y+ 2 doses, no booster"), or administer booster doses of the same vaccine product to 60+ years individuals ("10y+ 2 doses, 60y+ booster"), at the same pace, 6 months following dose 2. We further simulate the rollout of booster doses down to 40+ years, 20+ years, and 10+ years.

For the analysis in category 2 (LMIC and LIC countries with partial vaccine coverage), we aim to consider the relative impact of administering doses to vaccinate the younger working-age population with their primary series, versus diverting those doses to vaccinate the older population with a booster dose. We therefore construct two scenarios. In the first, we deliver the first two doses to the 60+ years population, at a maximum constant rate of 2% of the population receiving one dose per week, and assuming 80% uptake and delivery of the AZ vaccine. Once this coverage is achieved, vaccination is paused until the delay between administration of the second and booster doses (6 months) is complete. For the first scenario, we then vaccinate the 60+ years population with booster doses, beginning with the oldest (80+ years) age-group. For the second scenario, we take the same number of doses as would be required to give boosters to 60+ years, deliver these doses to individuals younger than 60 years (2 doses per person), again working downwards through the population until that dose supply is exhausted. We construct these rollout scenarios such that the number of doses given out each day is equivalent between scenarios with the total number of vaccines available sufficient to allow 80% coverage with 3 doses for the 60+ population.

For the category 3 analysis (minimal prior transmission in HIC and UMIC countries), we aim to quantify the impact of different strategies for lifting NPIs relative to vaccination coverage targets. We first simulated the impact of increasing R_t (to $R_t = 4$) once 80% coverage is achieved with primary immunisation (2 doses, around August 2021). We consider the total infections and deaths if vaccination continues such that no boosters are administered; if boosters are then targeted to 60+ years; or if boosters are targeted to 10+ years. In all scenarios, the vaccination rate is constant at 5% of the population dosed per week. Second, we simulated the impact of increasing R_t once the 60+ years population is boosted (around October 2021) and either stopping vaccination or continuing to

deliver boosters down to 10+ year age-groups. Finally, we simulate the impact of increasing R_t once boosters have been administered to the 10+ years population, assuming 90% uptake. We repeat these scenarios under the assumption that Omicron replaces Delta during November–December 2021; here we assume that if R_t has already increased to $R_t = 4$, then R_t further increases to 7.5. For the scenario where NPIs are not lifted until 2022, we assume a partial increase in R_t to 3.5 during the period of Omicron replacement, and the remaining increase to $R_t = 7.5$ in March 2022.

To model the impact of Omicron upon transmission and immune escape, we consider scenarios where Omicron is more transmissible than the Delta variant consistent with the rapid replacement observed in South Africa and the UK. The growth rate of the Omicron variant in the UK as of 13th December obtained from genotyping is estimated to be between 0.3 and 0.4 per day. This is compared to Delta for which the effective reproduction number in the presence of vaccine and infection-induced immunity was ~1 prior to the arrival of the Omicron variant. We parameterise our model with Rt in the absence of immunity, which we currently estimate to be in the region 2-4 worldwide. We therefore considered scenarios with R_t increasing from late November, gradually replacing Delta over a period of 4 weeks, to reach either 5 or 7.5. Over this same time period we reduce fold reductions in antibody titres such that the estimated vaccine efficacy against circulating virus reaches the levels in Table 1 once Omicron has fully replaced Delta.

Assumptions about setting characteristics and vaccine rollout are summarised in Table S2. As sensitivity analyses, we further consider scenarios with a period of 12 months between dose 2 and the booster dose, and scenarios with a slower vaccine rollout.

Table S2: Default scenarios and assumptions for the three broad modelled categories of country and epidemiological state. Values in parentheses represent sensitivity analyses.

	Income setting	HIC/UMIC	LMIC/LIC
Setting	Health system constraints	Unconstrained	Constraints present
	Contact patterns	HIC exemplar	LMIC exemplar
	Demography	HIC median	LMIC median
Vaccine characteristics	Product	Pfizer	Oxford-AstraZeneca
	Efficacy	See Table S1	See Table S1
	Short-term durability	Fitted (see Table S1)	Fitted (see Table S1)
	Long-term durability	Fitted (see Table S1)	Fitted (see Table S1)
Timing of roll-out and doses	Vaccine start date	1 January 2021	1 January 2021
	Timing of dose 2	28 days post-dose 1	28 days post-dose 1
	Timing of booster dose	180 days post-dose 2 (360 days)	180 days post-dose 2 (360 days)
	Vaccination rate	5% per week (2.5% per week)	2% per week (1% per week)
Vaccine targeting	Uptake	90%	80%
	Allocation	See Methods	See Methods

Each model run was performed with a simulation size of one million, across 10 random seeds, and the median and upper and lower 95% credible intervals summarised from the raw model outputs. We used these outputs to calculate the daily number of infections and deaths from 1 February 2020 to 31 December 2022, for each of the scenarios considered, as well as the total numbers of infections and deaths from the beginning of vaccine rollout (1 January 2021) to the end of the simulation window.
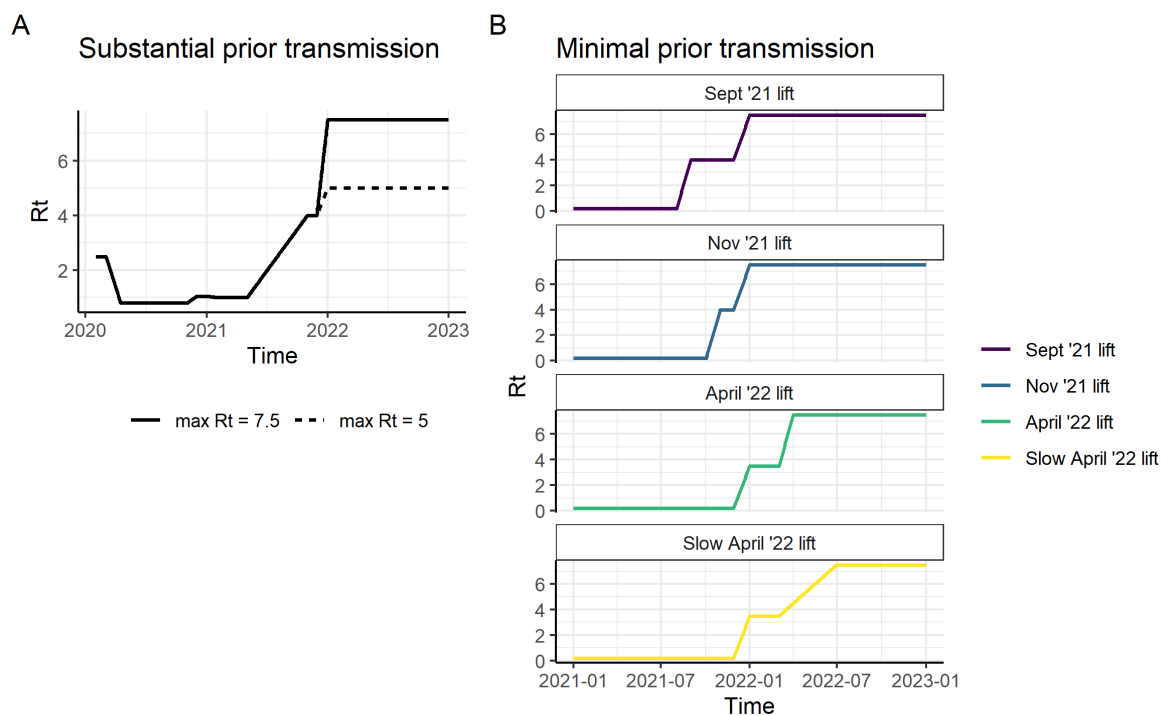

Figure S4: Modelled trajectories of the reproduction number R_t over time for (A) the settings with substantial prior transmission (categories 1 and 2); and (B) settings with minimal prior transmission, for the four R_t lifting scenarios (category 3).

9. Supplementary Results

Table S3: Estimated vaccine efficacy against mild disease, severe disease and death for the AZ-PF and PF-PF vaccine regimens as a function of time since dose 2 or booster made by fitting to vaccine efficacy estimates from a test-negative case control study in England(24, 25). Estimates are shown for the Delta variant and the Omicron variant. Values shown are the posterior median and 95% credible intervals. pd2 = post dose 2; pb = post booster.

Vaccine	Variant	90d pd2	180d pd2	30d pb	60d pb	90d pb
Efficacy against mild disease						
AZ-PF	Delta	54.6 (53.9-55.7)	35.4 (34.2-37.5)	92.2 (91.2-93.3)	90 (88.6-91.3)	87.2 (85.4-88.9)
AZ-PF	Omicron	17.5 (14.3-21.3)	8.8 (7.1-11.1)	67.7 (61.3-73.2)	61.3 (54.6-67.6)	54.6 (47.6-61.3)
PF-PF	Delta	76.6 (75.9-77.4)	59.9 (58.5-62)	92.2 (91.2-93.3)	90 (88.6-91.3)	87.2 (85.4-88.9)
PF-PF	Omicron	36.7 (31.1-42.1)	20.8 (17-25.1)	67.7 (61.3-73.2)	61.3 (54.6-67.6)	54.6 (47.6-61.3)
Efficacy against severe disease						
AZ-PF	Delta	90.8 (90.1-91.5)	81.7 (80.4-83.4)	99 (98.8-99.1)	98.7 (98.4-98.9)	98.2 (97.9-98.5)
AZ-PF	Omicron	63.4 (57.2-69.1)	44.1 (38.1-50.6)	94.5 (92.8-95.8)	92.8 (90.6-94.5)	90.7 (88-92.9)
PF-PF	Delta	96.4 (96-96.7)	92.4 (91.6-93.2)	99 (98.8-99.1)	98.7 (98.4-98.9)	98.2 (97.9-98.5)
PF-PF	Omicron	82.5 (78.3-85.8)	68.2 (62.3-73.4)	94.5 (92.8-95.8)	92.8 (90.6-94.5)	90.7 (88-92.9)
Efficacy against death						
AZ-PF	Delta	91 (89-92.8)	82.1 (78.7-85.5)	99 (98.7-99.2)	98.7 (98.3-99)	98.3 (97.8-98.7)
AZ-PF	Omicron	64.1 (56.3-71.4)	44.8 (37.1-53.5)	94.6 (92.5-96.2)	93 (90.3-95)	91 (87.6-93.5)
PF-PF	Delta	96.5 (95.6-97.2)	92.6 (90.9-94.1)	99 (98.7-99.2)	98.7 (98.3-99)	98.3 (97.8-98.7)
PF-PF	Omicron	82.9 (77.7-87.1)	68.8 (61.5-75.7)	94.6 (92.5-96.2)	93 (90.3-95)	91 (87.6-93.5)

Table S4: Sensitivity to estimated vaccine efficacy against mild disease, severe disease and death for the AZ-PF and PF-PF vaccine regimens as a function of time since dose 2 or booster. Assumes that after a booster the decay rate is half that post dose 2 and that the short period of decay is 5 days (i.e. most of the response is from long-lived plasma cells). Estimates are shown for the Delta variant and the Omicron variant. Values shown are the posterior median and 95% credible intervals. pd2 = post dose 2; pb = post booster.

Vaccine	Variant	90d pd2	180d pd2	30d pb	60d pb	90d pb
Efficacy against mild disease						
AZ-PF	Delta	54.8 (54.1-56.5)	44.8 (42.8-49.2)	88.7 (87.8-89.5)	86.8 (85.8-87.7)	84.8 (83.7-86)
AZ-PF	Omicron	15.2 (12.6-18.4)	10.7 (8.7-13.5)	53.5 (48.1-58.5)	49.1 (43.8-54.3)	45.1 (40-50.3)
PF-PF	Delta	75.3 (74.4-76.3)	67.1 (64.9-70.6)	88.7 (87.8-89.5)	86.8 (85.8-87.7)	84.8 (83.7-86)
PF-PF	Omicron	30.9 (26.3-35.8)	23 (19.2-28.1)	53.5 (48.1-58.5)	49.1 (43.8-54.3)	45.1 (40-50.3)
Efficacy against severe disease						
AZ-PF	Delta	88.5 (88.1-89.2)	83.7 (82.5-86)	98 (97.8-98.2)	97.6 (97.4-97.9)	97.2 (97-97.5)
AZ-PF	Omicron	53 (47.5-58.8)	43 (37.5-49.7)	87.9 (85.4-89.9)	85.9 (83.1-88.3)	83.8 (80.7-86.5)
PF-PF	Delta	95.1 (94.8-95.4)	92.8 (92.1-93.8)	98 (97.8-98.2)	97.6 (97.4-97.9)	97.2 (97-97.5)
PF-PF	Omicron	73.9 (69.1-77.9)	65.4 (59.9-71.1)	87.9 (85.4-89.9)	85.9 (83.1-88.3)	83.8 (80.7-86.5)
Efficacy against death						
AZ-PF	Delta	93.5 (93.2-93.9)	90.6 (89.7-92)	98.9 (98.8-99)	98.7 (98.6-98.8)	98.5 (98.4-98.7)
AZ-PF	Omicron	67.8 (62.8-72.8)	58.5 (52.9-65.1)	93.1 (91.6-94.4)	91.9 (90.2-93.4)	90.7 (88.7-92.3)
PF-PF	Delta	97.3 (97.1-97.5)	96 (95.6-96.6)	98.9 (98.8-99)	98.7 (98.6-98.8)	98.5 (98.4-98.7)
PF-PF	Omicron	84.1 (80.7-86.9)	78 (73.6-82.2)	93.1 (91.6-94.4)	91.9 (90.2-93.4)	90.7 (88.7-92.3)

Table S5: Sensitivity to estimated vaccine efficacy against mild disease, severe disease and death for the AZ-PF and PF-PF vaccine regimens as a function of time since dose 2 or booster. Assumes that the booster generates a 6-fold increase in NAT. Estimates are shown for the Delta variant and the Omicron variant. Values shown are the posterior median and 95% credible intervals. pd2 = post dose 2; pb = post booster.

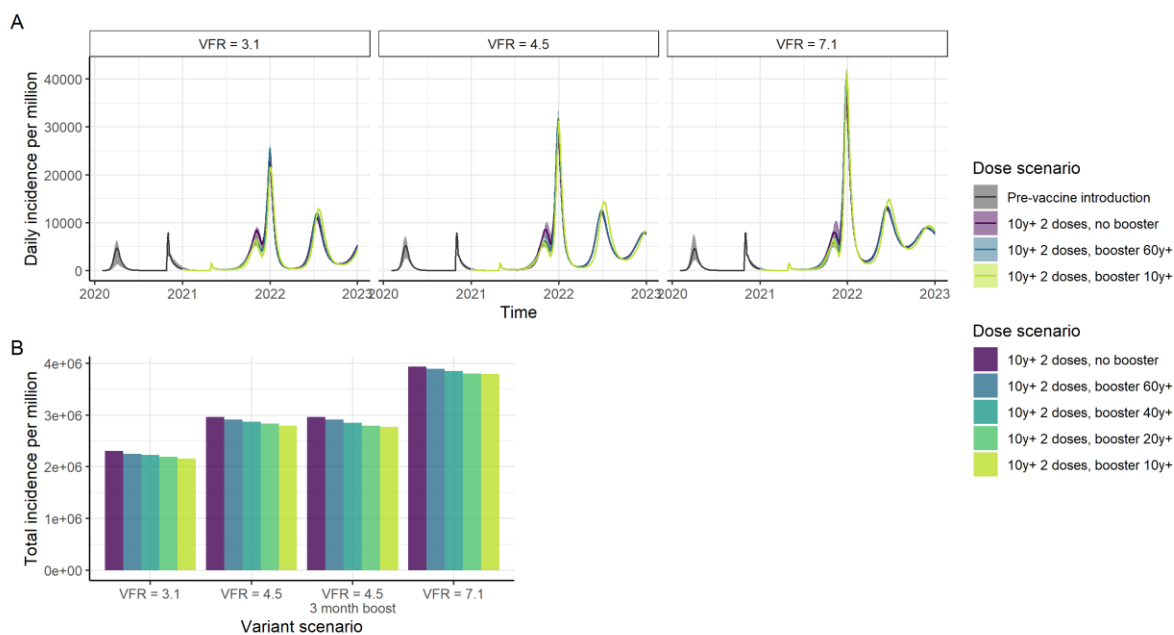| Vaccine	Variant	90d pd2	180d pd2	30d pb	60d pb	90d pb
Efficacy against mild disease						
AZ-PF	Delta	39 (37.9-40.6)	18.9 (17.3-22.2)	97.2 (95.4-98.5)	95.9 (93.4-97.8)	94.1 (90.7-96.7)
AZ-PF	Omicron	8.6 (7.1-10.6)	3.3 (2.7-4.4)	83.5 (74.4-90.8)	77.4 (66.5-87)	70 (57.6-81.9)
PF-PF	Delta	61.6 (60.2-62.9)	36.9 (34.3-41.3)	97.2 (95.4-98.5)	95.9 (93.4-97.8)	94.1 (90.7-96.7)
PF-PF	Omicron	19.1 (15.9-22.7)	7.9 (6.4-10.2)	83.5 (74.4-90.8)	77.4 (66.5-87)	70 (57.6-81.9)
Efficacy against severe disease						
AZ-PF	Delta	80.2 (79.4-81.3)	59.6 (57.1-64.3)	99.5 (99.2-99.8)	99.3 (98.9-99.6)	99 (98.4-99.5)
AZ-PF	Omicron	37.3 (32.3-42.9)	17.8 (14.8-22.4)	97 (94.8-98.4)	95.6 (92.6-97.7)	93.6 (89.5-96.6)
PF-PF	Delta	91 (90.5-91.5)	78.7 (76.7-81.7)	99.5 (99.2-99.8)	99.3 (98.9-99.6)	99 (98.4-99.5)
PF-PF	Omicron	59.8 (54.3-65.1)	35.2 (30-41.7)	97 (94.8-98.4)	95.6 (92.6-97.7)	93.6 (89.5-96.6)
Efficacy against death						
AZ-PF	Delta	88.3 (87.7-89.1)	73.4 (71.2-77.1)	99.8 (99.6-99.9)	99.6 (99.4-99.8)	99.5 (99.1-99.7)
AZ-PF	Omicron	52.6 (47.1-58.4)	28.9 (24.5-35.1)	98.3 (97.1-99.2)	97.6 (95.9-98.8)	96.5 (94.1-98.2)
PF-PF	Delta	95 (94.6-95.3)	87.4 (86-89.3)	99.8 (99.6-99.9)	99.6 (99.4-99.8)	99.5 (99.1-99.7)
PF-PF	Omicron	73.6 (68.9-77.7)	50.4 (44.6-57.4)	98.3 (97.1-99.2)	97.6 (95.9-98.8)	96.5 (94.1-98.2)

Figure S5: Impact of vaccination (incidence) in a high-income country setting with substantial prior transmission and high vaccine access. A) Daily incidence per million for the central, upper, and lower VFR values. B) Total incidence per million from vaccine introduction at the beginning of 2021 through to the end-2022 the three VFR values assuming Omicron replaces Delta during November–December 2021, and assuming a 6-month period between dose 2 and the booster, with an additional scenario showing the impact of assuming a 3-month period. Vaccine impact is shown for five scenarios: no booster doses, booster doses to those aged 60+, booster doses to those aged 40+, booster doses to those aged 20+ and booster doses to those aged 10+. All scenarios assume 90% vaccine uptake in each group and 90% of those aged 10+ receive the primary series.
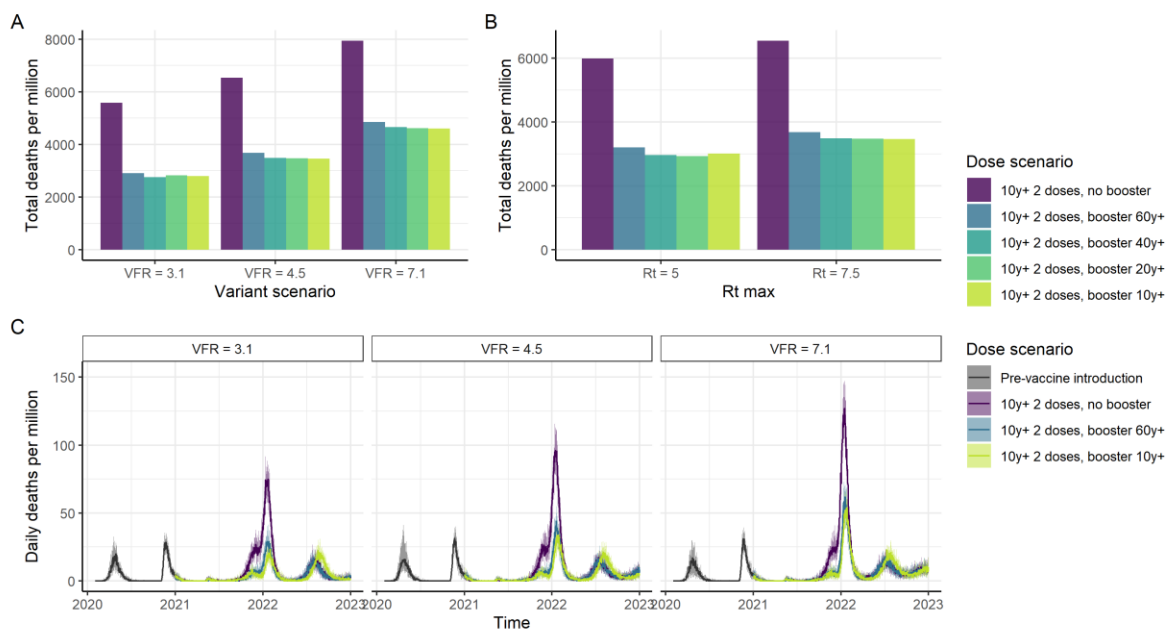
Figure S6: Sensitivity analysis to estimates of vaccine efficacy in a high-income country setting with substantial prior transmission and high vaccine access. Total deaths per million from vaccine introduction at the beginning of 2021 through to the end-2022 for the three VFR values assuming Omicron replaces Delta during November–December 2021, and assuming a 6-month period between dose 2 and the booster. Vaccine impact is shown for five scenarios: no booster doses, booster doses to those aged 60+, booster doses to those aged 40+, booster doses to those aged 20+ and booster doses to those aged 10+. All scenarios assume 90% vaccine uptake in each group and 90% of those aged 10+ receive the primary series.

Figure S7: Sensitivity analysis to estimates of vaccine efficacy in a high-income country setting with substantial prior transmission and high vaccine access. Uses vaccine efficacy estimates based on the assumption that the booster doses give protection associated with a 6-fold increase in NATs, where the resulting vaccine efficacy is shown in Table S5. A) Total deaths per million post vaccine introduction at the beginning of 2021 through to end-2022, for the central, upper, and lower VFR estimates, and assuming a 6-month period between dose 2 and the booster. B) Total deaths per million over the same period, for two scenarios for the increased transmissibility of the Omicron variant (expressed as the maximum R_t) for our central estimate of immune escape of the Omicron variant. C) Daily deaths per million for the lower, central, and upper VFR estimate and assuming R_t reaches 7.5. Vaccine impact is shown for five scenarios: no booster doses, booster doses to those aged 60+, booster doses to those aged 40+, booster doses to those aged 20+ and booster doses to those aged 10+. All scenarios assume 90% vaccine uptake in each group and 90% of those aged 10+ receive the primary series.
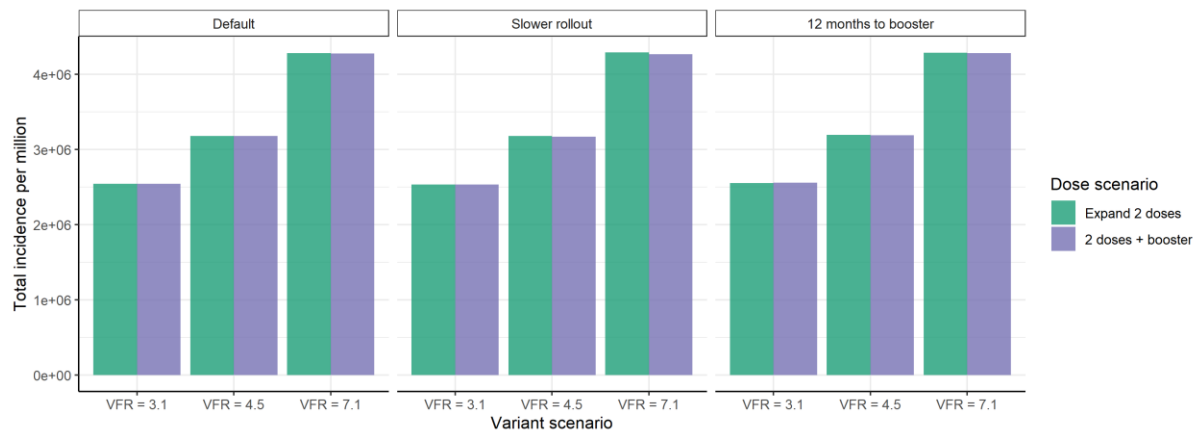
Figure S8: Impact of vaccination (total incidence) in a low-middle-income country setting with substantial prior transmission and low vaccine access, assuming the population 60+ years is initially targeted. Two strategies for distributing a fixed limited supply are shown. In the first ("Expand 2 doses"), no booster doses are administered, and the supply is therefore delivered to a wider proportion of the population. In the second ("2 doses + booster") the same supply is delivered to the 60+ age-group (2 dose primary immunisation and booster dose 6 months post dose 2) and no younger groups receive the primary series. The bars show total incidence per million population from vaccine introduction in 2021 to end-2022, for the central, upper, and lower VFR estimates, and assuming R_t reaches 7.5, as Omicron replaces Delta during November–December 2021. Total incidence is shown for the default vaccine rollout (2% of the population per dose per week) and default booster dose timing scenario (180 days post dose 2, "Default"), as well as assuming a slower rollout (1% per week, "Slower rollout") or a one-year gap between dose 2 and the booster ("12 months to booster").
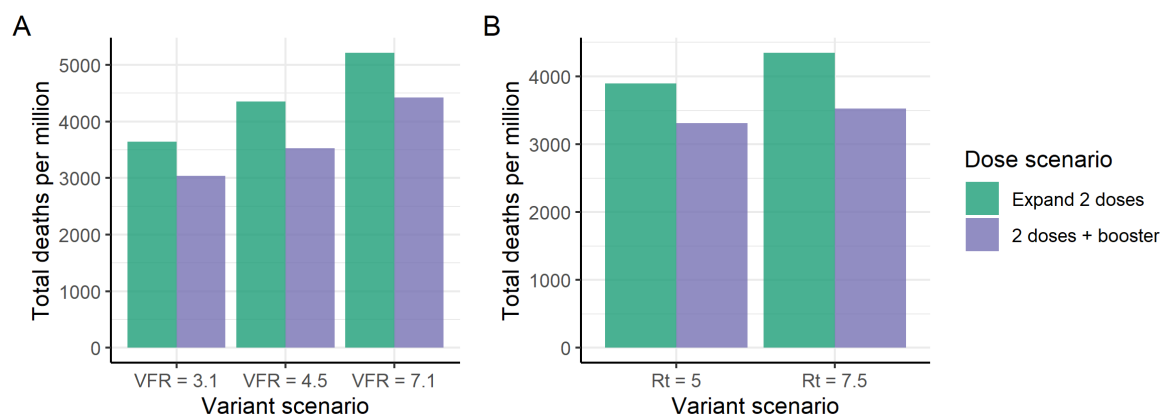

Figure S9: Sensitivity analysis to estimates of vaccine efficacy in a high-income country setting with substantial prior transmission and high vaccine access. Uses vaccine efficacy estimates based on the assumption that the booster doses give protection associated with a 6-fold increase in NATs, where the resulting vaccine efficacy is shown in Table S5. A) Total deaths per million population from the start of vaccination in 2021 to end-2022 for the three VFR parameters, assuming the default vaccine rollout (2% of the population per dose per week) and booster dose scenario (180 days post dose 2). B) Total deaths per million over the same period, for two scenarios for the increased transmissibility of the Omicron variant (expressed as the maximum Rt) for our central estimate of immune escape of the Omicron variant.
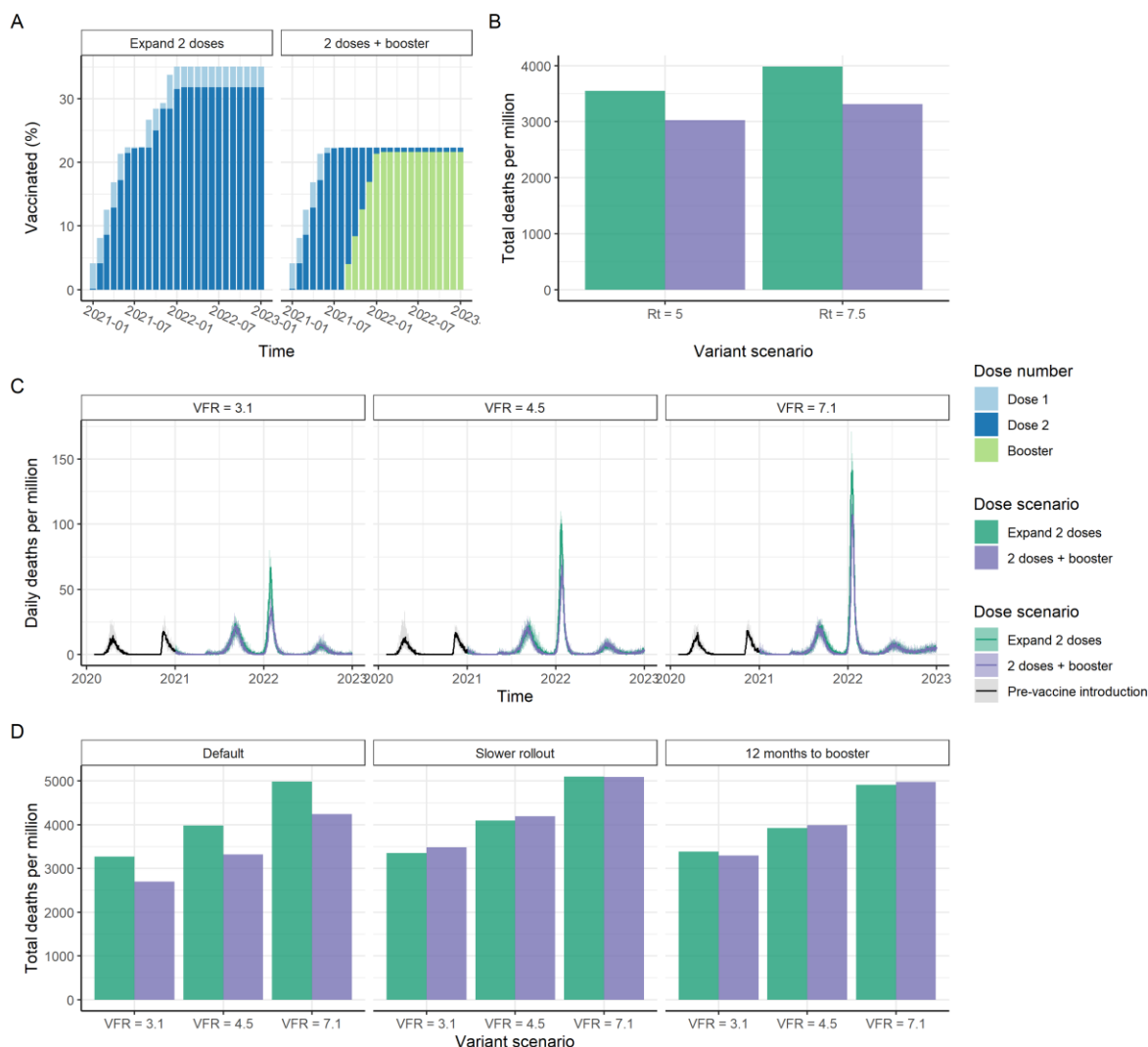
Figure S10: Impact of vaccination in a low-middle-income country setting with substantial prior transmission and low vaccine access, where individuals 40+ years are targeted. Two strategies for distributing a limited vaccine supply are shown. In the first ("Expand 2 doses"), no booster doses are administered, and the supply is therefore delivered to a wider proportion of the population. In the second ("2 doses + booster") the same supply is delivered to the 60+ age-group (2 dose primary immunisation and booster dose 6 months post dose 2) and no younger groups receive the primary series. A) Cumulative proportion of the population having dose 1 (light blue), dose 2 (dark blue) and the booster (green) each month. B) Total deaths per million from vaccine introduction at the beginning of 2021 through to end-2022, for two scenarios for the increased transmissibility of the Omicron variant (expressed as the maximum Rt) for our central estimate of immune escape of the Omicron variant. C) Daily deaths per million population assuming R_t increases to 7.5. for the central, upper, and lower VFR estimates. D) Total deaths per million population from the start of vaccination in 2021 to end-2022 for the three VFR parameters. Total deaths are shown for the default vaccine rollout (2% of the population per dose per week) and booster dose scenario (180 days post dose 2, "Default"), as well as assuming a slower rollout (1% per week, "Slower rollout") or a one-year gap between dose 2 and the booster ("12 months to booster"). Results for the scenario where the 60+ years population is initially targeted are shown in Figure 3.
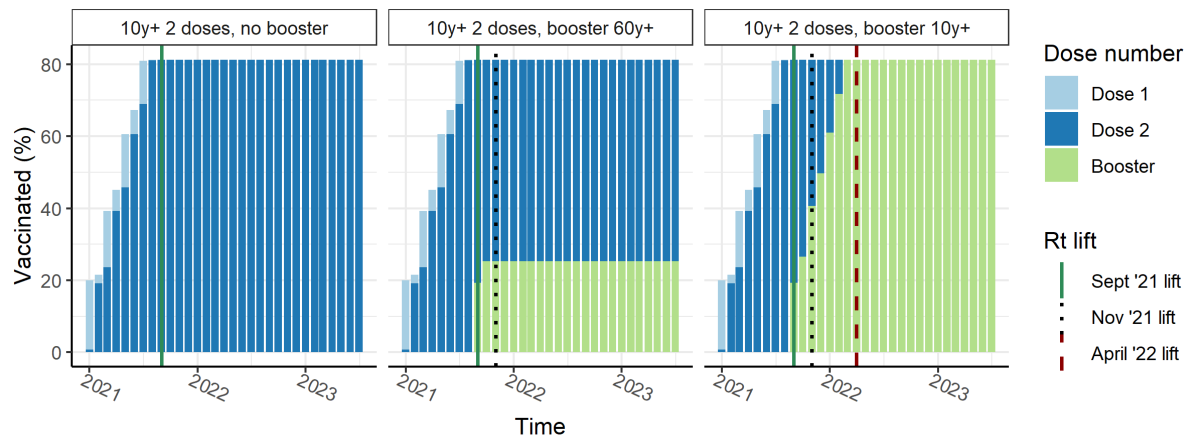
Figure S11: Percentage of the population vaccinated with either one dose (light blue bars), two doses (dark blue), or two doses plus a booster dose (light green), per month from January 2021 for the high-income country setting with high vaccine access and minimal prior transmission (category 3 analysis). The vertical lines show the different options for lifting NPIs (i.e. increasing R_t) relative to the rollout of vaccine doses. The "Sept '21 lift" corresponds to lifting NPIs after 80% of the population has received two doses; "Nov '21 lift" corresponds to lifting following rollout of booster doses to the 60+ years population; and "April '22 lift" corresponds to lifting after boosters have been rolled out to the 10+ years population. The population health impact for these roll-out and lifting scenarios is in Figure 4.
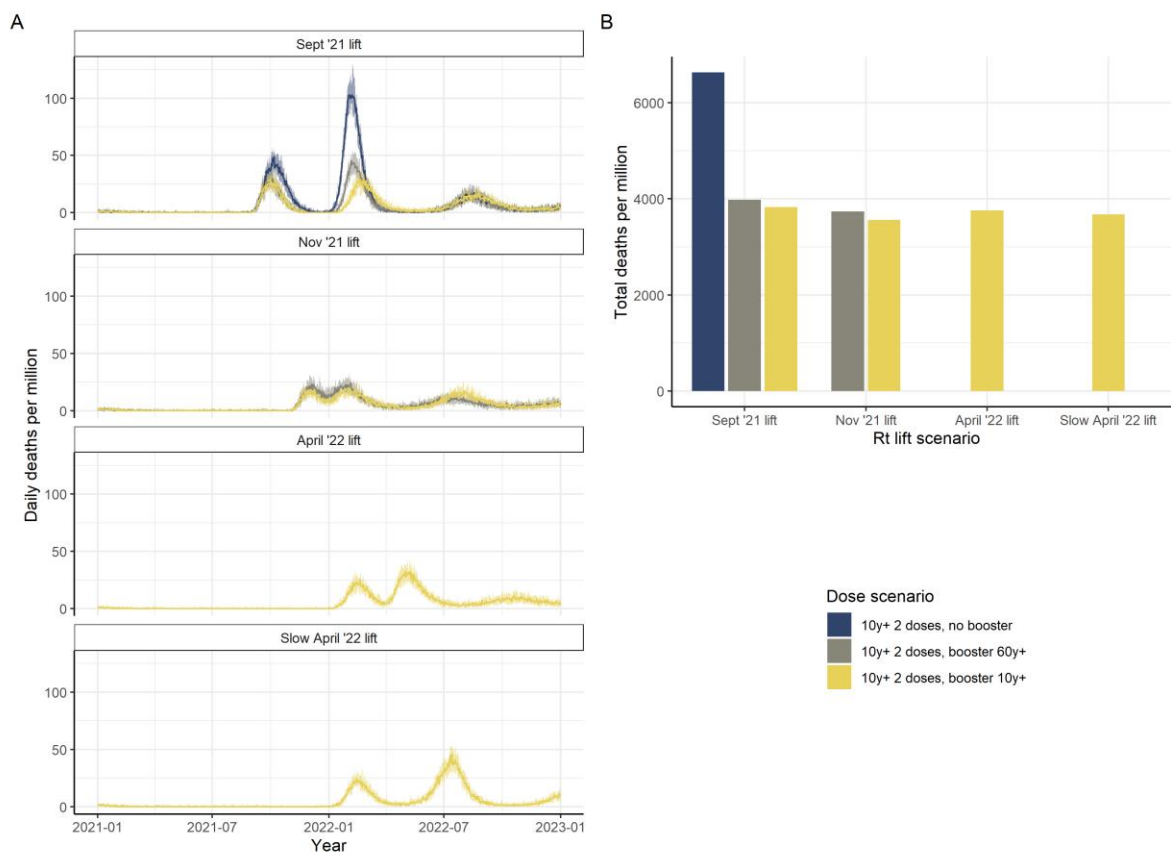
Figure S12: Sensitivity analysis to estimates of vaccine efficacy in a high-income country setting with minimal prior SARS-CoV-2 transmission and high vaccine access. Uses vaccine efficacy estimates based on the assumption that the booster doses give protection associated with a 6-fold increase in NATs, where the resulting vaccine efficacy is shown in Table S5. A) Daily deaths per million population for the scenario where 80% of the population is immunised (2 doses) before NPIs are lifted (i.e. R_t increases). Following Rt increasing ("Sept '21 lift"), vaccination continues at a population dose rate of 5% per week until 90% uptake is achieved in the 10+ years population (brown); boosters are administered to the 60+ years population 6 months post dose 2 (dark blue); or boosters are administered to the 10+ years population (yellow). Additional panels show the impact of lifting NPIs after boosters are given to 60+ years ("Nov '21 lift") or after boosters are given to 10+ years ("April '22 lift" representing a lifting over a one-month period; "Slower April '22 lift" representing lifting over a four-month period). The central VFR estimate and a maximum transmission of $R_t = 7.5$ are applied. B) Total deaths per million population from the start of vaccination in 2021 to end-2022, for each scenario.